Sl. No.	**IIT Ropar** **List of Recent Publications with Abstract** **Coverage: January, 2025**
A	**Book Chapter(s)**
1.	Application of nanotechnology in antimicrobial coating on surgical instruments **P Yadav, M Kamboj, B Das** - Applications of Nanotechnology in Biomedical Engineering: Book Chapter, 2024 **Abstract:** Surgical site infections (SSIs) are among the most prevalent nosocomial disorders that can cause significant consequences following surgical procedures. SSIs place a tremendous physical, psychological, and financial strain on the patients and medical personnel. SSI infections persist as a substantial factor in mortality and morbidity following surgery. The most frequent cause of postoperative infections is bacterial pathogens, which include both Gram-positive and Gram-negative bacteria. With a variety of exposure methods, such as the surface of contaminated surgical instruments, these bacteria can contaminate a surgical wound site. Biomedical equipment including implants or surgical sutures, also provides the optimal locations for bacterial adhesion, colonization, and biofilm development. In the last decade, antibacterial coatings have progressively become a crucial component of the global strategy to prevent the spread of microbial pathogens. The increased knowledge and understanding of nanotechnology have led to a wide range of coating alternatives that imbue surfaces of biomedical and surgical equipment with antimicrobial and antibiofilm qualities. The significant concurrent improvements in biotechnology, materials science methodologies, and the affordability of coating processes assist in avoiding bacteria proliferation by imparting multifunctionality and enhancing the long-term stability of the surface. To proceed toward a more structured approach in this fascinating but challenging area, we summarize and evaluate the primary nanoparticles used for coating the surgical tools, their antibiofilm actions and mechanisms, and the popular methods for these nanoparticles on the surface of the tools. Finally, we provide an overview of the applications of implants and surgical tools with nanoparticle-based antimicrobial coating.
B	**Conference Proceeding(s)**
2.	Aberration laser beams with controlled autofocusing, self-healing and intensity distribution **V Dev, V Pal** - Advances in Photonics Integrated Circuits, LASER and Applications, (PHOTONICS 2023), 2025 **Abstract:** We investigate the aberration laser beams (ALBs) with controlled autofocusing, self-healing and spatial intensity distribution, in free space as well as in turbulent media. ALBs are generated with a diffractive optical element, whose phase distribution consists of radial and periodic angular dependence. The ALBs possess autofocusing properties, and the autofocusing distance can be controlled by the parameters of ALB. The turbulence causes the beam to wander and deteriorates its spatial shape. However, the autofocusing properties remain invariant. Furthermore, we demonstrate that ALBs are capable of self-healing against the obstructions in free space as well as in turbulent media. The propagation distance needed for self-healing is found to be independent of amount of blocking, and maximum self-healing occurs at the autofocusing distance. Further, we show that by introducing asymmetry in the phase distribution of ALB, its intensity can be controlled precisely, which generates high-power densities.
3.	AC conductivity measurement of conductor sleeves **R Kumar, P Johri, P Sharma, CC Reddy** - 2024 IEEE 7th International Conference on Condition Assessment Techniques in Electrical Systems (CATCON), 2025

	Abstract: The use of overhead covered conductors and conductor sleeves plays a crucial role to provide insulation and safety from the environmental hazards in the power systems. Covered conductors have a rigid insulation layer over a bare conductor, which restricts their flexibility especially in hilly areas or wherever the sharp turn is required. In contrast, conductor sleeves offer a more flexible structure, allowing their easy installation, replacement if required, and are cost-effective. However, investigation of the optimal design of conductor sleeves requires an accurate measurement of the AC conductivity. In this paper, an experimental setup and its methodology for the measurement of AC conductivity on the surface and in the interface of conductor sleeves is proposed. Additionally, dielectric spectroscopy has been performed to determine volumetric AC conductivity.
4.	AppleV: A dataset for apple fruit volume estimation **S Barda, Aditya, R Kinha, N Goel** - ICVGIP'24: Proceedings of the Fifteenth Indian Conference on Computer Vision Graphics , 2024 **Abstract:** The apple is among the most widely consumed fruits globally due to its high nutritional value and longer shelf life. Consequently, there is a need to monitor post-harvest health, which has important applications in grading, packaging and transportation. These tasks require the accurate computation and prediction of fruit size; however, there is a lack of publicly available datasets that the researcher can use to generalize it over apples. To bridge this gap, we introduce the AppleV dataset, which consists of images of 200 apples taken from different angles and sums up to 2000 images with their corresponding volume measurement. This work also explores three traditional approaches(Analytical method, Support Vector Machine Regression(SVMR), and Dynamic weighting) and five deep learning approaches(Custom model, EfficientNetV2S, VGG16, Xception, and ResNet50) for volume estimation. Traditional approaches use handcrafted features to estimate volume, whereas deep learning approaches learn these features automatically. To mitigate the risk of overfitting caused by the large number of trainable parameters in state-of-the-art deep learning models, pre-trained models trained on the ImageNet dataset are utilized. The results indicate that while the custom model demonstrated superior performance on the training data, ResNet50 outperformed all other methods on the AppleV dataset in terms of validation data accuracy. This work tries to offer a standard dataset specifically for the volume estimation task and aims to advance agricultural technology by automating volume estimation for apples based on image data, facilitating improved quality assessment and has various applications in industries such as grading and sorting.
5.	Development of CNN-based model for mango leaf disease classification S Utomo, MI Devi, **A Pratap**… - 2024 IEEE International Conference on Smart Mechatronics (ICSMech), 2024 **Abstract:** Food security has become an urgent topic that needs more focus. It is one of 17 sustainable development goals. Specifically, SDG 2: zero hunger. We need effective solutions from multidisciplinary domains to achieve this goal. The advancement and growth of artificial intelligence could also provide a promising solution to achieving zero hunger. This paper proposes a solution to promote sustainable agriculture practices. We chose the classification of mango leaf disease as our case study. We successfully develop an accurate and efficient convolutional neural network-based model as a solution. The proposed model achieved 99.5% accuracy and outperformed the majority state-of-the-art models, only losing to DeiT, which achieved 99.75% accuracy. However, the proposed model comes with 739,080 parameters, which are 4.73 and 115.95 times smaller than MobileNetV2 and DeiT, respectively. We believe this finding could assist farmers in accurately classifying mango leaf disease, thereby enabling timely and precise preventive action. This leads to a decrease in material loss and the preservation of plant productivity. Leveraging this achievement, forthcoming initiatives seek to disseminate these technologies across multiple plant diseases.

6.	Effect of amplitude-phase coupling on the formation of dissipative topological defects in coupled lasers **S Sahoo**, S Karuseichyk…**V Pal** - Advances in Photonics Integrated Circuits, LASER and Applications, (PHOTONICS 2023), 2025 **Abstract:** Finding a globally stable defect-free state can be exploited for solving computationally hard optimization problems, which occur in a wide range of fields. We present the effect of amplitude-phase coupling (linewidth enhancement factor, α) on the formation of dissipative topological defects in a one-dimensional ring array of coupled lasers. We have found that the probability of topological defects (ρ) depends on several parameters, such as system size (number of lasers (N)), amplitude-phase coupling, coupling strength, and pump strength. Specifically, it increases monotonically with the system size. It is also found to be the lowest for a large amplitude-phase coupling factor. The probability of topological defects decreases significantly when the lasers operate close to the threshold. For different types of coupling between the lasers, the relation for the probability of topological defects is found as $\rho_{NN} > \rho_{NU} > \rho_{NNN}$.
7.	Effect of curing on the AC and DC breakdown strength of cable insulation **SM Anas, HK Azmeera, CC Reddy** - 2024 IEEE 7th International Conference on Condition Assessment Techniques in Electrical Systems (CATCON), 2025 **Abstract:** Cross-linked polyethylene (XLPE) is one of the most used insulation materials in the cable manufacturing industry due to its excellent properties compared to other insulating materials. The manufacturing of XLPE cable involves the curing process where the insulation is subjected to a high temperatures and pressures for a certain defined duration in order to ensure the proper crosslinking and thereby enhance the material's performance. In this paper, lab-made XLPE samples are subjected to different curing temperatures (uncured, 150°C, 180°C and 200°C) in order to investigate breakdown characteristics under both AC and DC conditions. A possible optima for temperature, where the insulation is properly cross-linked but not deteriorated, is touched upon briefly. The results, albeit preliminary, will be a good starting step, which will hopefully guide the industry in improving the efficiency and reliability of the cable.
8.	Effect of insulation bulging on the electric field distribution in AC cables **P Mishra, P Johri, P Sharma, CC Reddy** - 2024 IEEE 7th International Conference on Condition Assessment Techniques in Electrical Systems (CATCON), 2025 **Abstract:** This paper presents the effect of bulging on the electric field distribution of an AC cable. Bulging is a type of deformation or defect, where the cable undergoes swelling or expansion in a certain area, resulting in a non-uniform geometry. This may occur due to various reasons such as mechanical stress, thermal stress, overloading, excessive bending, and sometimes environmental factors. The effect of the extent of bulging has been investigated in a finite element method (FEM) based model with electro-thermally coupled simulations. The results are expected to provide useful insights into the design and operational aspects of the cables.
9.	Effect of thermal stress on MV cable insulation **HK Azmeera, SM Anas, CC Reddy** - 2024 IEEE 7th International Conference on Condition Assessment Techniques in Electrical Systems (CATCON), 2025 **Abstract:** Effect of thermal stress on the XLPE insulation in underground power cables plays a significant role in determining the life of the cable. In this study two widely used medium voltage cable insulations are thermally aged at three different temperatures for a duration of 12months (8760 hours). The morphological changes are studied using FTIR and XRD tests and the electrical changes are determined by dielectric breakdown tests. The material with better thermal performance is determined based of the analysis. This work helps in assessing the material best suited for medium voltage applications.
10.	Evolving safety protocols: Deep learning-enabled detection of personal protective equipment

	M Alahmid, K Bhimani…**S Ghildiyal**… - International Conference on Computer Vision, High-Performance Computing, Smart Devices and Networks (CHSN 2023), 2024 **Abstract:** To give shift in safety protocols, we have employed advanced deep learning algorithms and frameworks (Shrestha and Mahmood in IEEE Access 7:53,040–53,065, 2019 [25]) to construct an innovative AI model. The designed model detects the usage of personal protective equipment (PPE) (Personal protective equipment. Geneva: World Health Organization, 2020 [18]) by workers in high-risk industries such as construction and manufacturing. We have used Google's TensorFlow object detection API (Sai and Sasikala in Object detection and count of objects in image using tensor flow object detection API, pp 542–546, 2019 [22]) to modify and train a model for dual purposes: PPE detection and face recognition. The state-of-the-art of this research is to substantially enhance safety compliance by addressing the prevalent issue of PPE non-compliance. To emphasis this, we have developed a pioneering software prototype that synergizes PPE detection with a face recognition-based clock-in system. This prototype demonstrates impressive object detection metrics with a mean average precision (mAP) of 0.9 for vests and 0.85 for helmets. Moreover, it exhibited efficient face recognition with a successful threshold range of 17–20%. The implementation of AI in our system promises significant enhancements to worker safety, while concurrently reducing the financial burden associated with big hazards and accidents. Beyond the development and performance of the system, this paper provides a thorough exploration of the encountered challenges, potential real-world applications (particularly in employee monitoring and clock-in systems), and the future implications of this study on research and practical applications in the field of AI-integrated safety compliance.
11.	Fortifying artificial pancreas: A hardware-in-the-loop simulation study of cyber-attacks and defense mechanisms Vaibhav, S Saxena, S Bhatia, **N Kumar** - 2024 15th International Conference on Computing Communication and Networking Technologies (ICCCNT), 2024 **Abstract:** Artificial Pancreas (AP) is a recent technology developed to aid type-1 diabetic patients in maintaining their recommended blood glucose levels. It mimics the function of the natural pancreas by continuously monitoring the patient's blood sugar level and delivering an adequate amount of insulin to their body. AP is a closed-looped system involving several device components communicating over wireless protocols. Anomalous behavior of any device component or communication protocol due to a cyber-attack can be life-threatening. Hence, it is essential to make the AP system resilient against cyber-attacks. This paper presents the development of a hardware-in-the-loop (HIL) simulation of AP using the Bergman Minimal Model (BMM), which is then used to simulate the responses of two common but potentially catastrophic (to the patients' health) cyber-attacks, viz., template attack and denial-of-service (DoS) attack. The paper also presents the development of detection and mitigation algorithms against these attacks.
12.	High-power orbital angular momentum modes obtained by phase-locking lasers in a 1D ring array **V Dev, V Pal** - Advances in Photonics Integrated Circuits, LASER and Applications, (PHOTONICS 2023), 2025 **Abstract:** We investigate the generation and propagation of high-power orbital angular momentum (OAM) modes by a phase-locking one-dimensional (1D) ring array of lasers. Such OAM modes are also referred to as discrete vortices. Phase locking enables the generation of high-power vortices, as several lasers are locked to generate a single high-power beam. The lasers are phase-locked in a desired phase configuration (OAM modes) by adding spatial Fourier filtering, through a specifically designed amplitude mask, inside a degenerate cavity. Unlike continuous vortices (Laguerre-Gaussian/Bessel beams), for a given system size and fixed inter-laser separation, the divergence of a discrete vortex does not depend on the orbital angular

	momentum (or topological charge). Further, we show that the discrete vortices also exhibit good self-healing properties against different kinds of obstructions in the waist plane (z = 0) as well as in the propagation plane (z > 0).
13.	Influence of openings on seismic failure mechanism of URM infilled RC hill buildings **Z Naorem, P Haldar** - The International Conference on Net-Zero Civil Infrastructures: Innovations in Materials, Structures, and Management Practices (NTZR 2024), 2025 **Abstract:** Seismic risk associated with the hilly and mountainous region of the Indian Himalayas is immensely high owing to a combination of the extremely high seismicity of the region and the vulnerability of the irregular buildings constructed on sloping terrain. Scientific studies on the seismic vulnerability of such buildings are performed on either bare frame or fully infilled buildings without considering openings in the infill panels for doors and windows. However, presence of openings plays an important role in the overall seismic performance. The present study aims to understand the effects of openings on the dynamic properties of unreinforced masonry (URM) infilled RC buildings constructed on sloping terrains such as the modal properties and fundamental period of vibration. Various opening ratios are considered as per construction practices in India, and the dynamic properties are compared with those of fully infilled buildings. A comparison of dynamic properties revealed that the period of vibration increases and the modal participation ratio corresponding to the fundamental mode of vibration decreases with an increase in the opening ratio. The displacement at the roof of the buildings was also found to increase with an increase in the opening ratio and the maximum displacement was found to be 25–63% higher as compared to fully infilled buildings depending on the opening ratio. Non-linear dynamic analysis has been performed to identify and compare key structural parameters responsible for the collapse of hill buildings with varying opening ratios.
14.	Intelligent diagnosis of transformer faults using DGA **A Dhiman, HK Azmeera, CC Reddy** - 2024 IEEE 7th International Conference on Condition Assessment Techniques in Electrical Systems (CATCON), 2025 **Abstract:** Power transformers are the most crucial components of an electrical power system, and their reliable operation is essential for maintaining a continuous power supply. The conventional IEC three-ratio method has been used for the incipient faults detection in power transformers by analyzing dissolved gas concentrations based on DGA results. However, accurate fault classification based on the conventional IEC method can be found challenging when the measured gas ratio is slightly diverged from the crisp boundaries of ranges assigned by this method. The paper proposes a novel approach to overcome the drawbacks by integrating artificial neural networks (ANNs) and classifiers with DGA data. The effectiveness and robustness of the proposed approach are confirmed by the simulation results of both techniques, which show that the proposed method is able to provide high prediction and reliable diagnosis for the identification of transformer faults.
15.	Investigation of sheath current at different joints for different types of bonding during busbar fault **A Das, SM Anas, CC Reddy** - 2024 IEEE 7th International Conference on Condition Assessment Techniques in Electrical Systems (CATCON), 2025 **Abstract:** Cable sheath provides shielding against moisture ingress and provides mechanical support to the insulation. However, due to current flowing in the conductor and phase voltage an induced current flows through the sheath, which degrades the cable's lifespan and potentially causes cable failures. Along with this, additional transients like busbar faults will degrade the condition of the insulation. For the energy distribution between the feeders, busbars are utilized and any fault in the busbar can lead to disruption in the power delivery. So, to ensure safety, a close monitoring of sheath current during busbar fault is important and this proactive approach helps to prevent further serious problems. In this paper, simulations are carried out to find the

	sheath current in different joints during busbar faults for different types of bonding.
16.	Investigation on cable breakdown using aluminium foil as electrode **P Sharma, R Kumar, CC Reddy** - 2024 IEEE 7th International Conference on Condition Assessment Techniques in Electrical Systems (CATCON), 2025 **Abstract:** The use of power cables has increased enormously due to several advantages such as safety, durability, reliability, and quality of power supply without any interruption. To maintain these features, there needs to be proper testing of cable before use. This research paper presents a comprehensive and cost-effective method for the testing of cable. In this paper authors investigated three different method for the testing of cable experimentally and further simulated using FEM based software and concluded the best among three.
17.	Investigations on the revision in the eccentricity limits to improve the performance of extruded HVDC cables **P Johri, CC Reddy** - 2024 IEEE 7th International Conference on Condition Assessment Techniques in Electrical Systems (CATCON), 2025 **Abstract:** This paper highlights the problems associated with a prevalent defect in extruded HVDC cables called eccentricity, which refers to an uneven thickness of insulation in the cable cross-section. IEC 62067 specifies an upper limit of 10% on the allowed eccentricity. However, this limit needs to be revised owing to the electro-thermal instability concerns, as discussed in this paper. Based on comprehensive electro-thermal FEM simulations, the authors investigate the effect of eccentricity under different operating conditions of the cable and thereby suggest appropriate revision to the standard.
18.	Location of Damaged Insulation for an Underground Power Cable Under High-Frequency Model **A Das, CC Reddy** - 2024 IEEE 7th International Conference on Condition Assessment Techniques in Electrical Systems (CATCON), 2024 **Abstract:** This paper proposes a novel broadband impedance spectroscopy through a sweep frequency response analysis approach for estimating the position of damaged insulation, particularly the site of water treeing. Water treeing is an undiagnosed issue in cables that does not result in a partial discharge until a catastrophic failure happens. Therefore, an attempt was made to pinpoint this kind of cable damage using impedance spectroscopy in this research. In addition, an analytical method based on the frequency location of zeros and their cumulative total and product is suggested for estimating the location of water treeing of different sizes in the insulation. To validate the suggested equations, tests were conducted on the test cable to generate water treeing based on a model based on the literature.
19.	Low-profile orthogonal-ports dual-polarized antenna for full-duplex WBAN applications **A Thakur, A Sharma** - 2024 15th International Conference on Computing Communication and Networking Technology (ICCNT), 2024 **Abstract:** A low-profile orthogonal-ports dual-polarized antenna is presented for WBAN applications within the 5.8GHz ISM-band. The antenna, designed on RT/duroid 5880 semi-flexible substrate, achieves dual-polarization using orthogonal-ports with cross-polarization discrimination better than ~25 dB, making it suitable for full-duplex applications. To test the antenna's robustness, it is simulated on a human body model and exhibits a maximum SAR of 0.2639W/Kg, validating compliance with safety standards. Operating across the frequency range of 5.725−5.875GHz, the antenna functions reliably in both free space (FS) and on body (OB) scenarios, with isolation better than 31dB and 29.45dB, respectively. Peak simulated gains of 7.55 dBi and 5.53dBi are observed in the FS and OB, respectively. These features render the proposed design an ideal choice for full-duplex WBAN applications.
20.	Mobile agents on Chordal graphs: Maximum independent set and beyond

	T Kaur, K Paul, K Mondal - Distributed Computing and Intelligent Technology (ICDCIT), 2025 **Abstract:** We consider the problem of finding a maximum independent set (MaxIS) of chordal graphs using mobile agents. Suppose *n* agents are initially placed arbitrarily on the nodes of an *n*-node chordal graph $G=(V,E)$. Agents need to find a maximum independent set *M* of *G* such that each node of *M* is occupied by at least one agent. Also, each of the *n* agents must know whether its occupied node is a part of *M* or not. Starting from both rooted and arbitrary initial configuration, we provide distributed algorithms for *n* mobile agents having $O(log\ n)$ memory each to compute the MaxIS of *G* in $O(mnlog\Delta)$ time, where *m* denotes the number of edges in *G* and Δ is the maximum degree of the graph. Agents do not need prior knowledge of any parameters if the initial configuration is rooted. For arbitrary initial configuration, agents need to know few global parameters beforehand. We further show that using a similar approach it is possible to find the maximum clique in chordal graphs and color any chordal graph with the minimum number of colors. We also provide a dynamic programming-based approach to solve the MaxIS finding problem in trees in $O(n)$ time.
21.	Path connected dynamic graphs with a study of efficient dispersion **A Saxena, K Mondal** - ICDCN'25: Proceedings of the 26th International Conference on Distributed Computing and Networking, 2025 **Abstract:** In dynamic graphs, usually, several edges may get added or deleted in a round with respect to the previous round. There are different connectivity models based on the constraints on the addition/deletion of edges. One such model is known as *T*-Interval Connectivity model where edges can be added/deleted keeping the graph nodes connected in each synchronous round. The parameter *T* depends on the stability of the underlying connected structure across rounds. There is another connectivity model for dynamic graphs, namely Connectivity Time model where the union of all the edges present in any *T* consecutive rounds must form a connected graph. This is much weaker than the *T*-Interval Connectivity as the graph may even be disconnected at each round. We, in this work, come up with a new connectivity model, namely *T*-Path Connectivity. According to our model, the nodes may not remain connected in each round, but for any pair of nodes *u*, *v*, there must exist path(s) at least once in any consecutive *T* rounds. We show that our model is weaker than *T*-Interval Connectivity but stronger than Connectivity Time model. We study the dispersion problem of mobile agents on our connectivity model. Dispersion is already studied in the *T*-Interval Connectivity model for $T = 1$. We show that the existing algorithm in 1-Interval Connected graphs for dispersion with termination does not work in our model for obvious reasons. We answer what are the necessary assumptions to solve dispersion in our connectivity model. Then we provide an algorithm that runs in optimal time and memory with those minimal model assumptions on *T*-Path Connected dynamic graphs. Also, we show that solving dispersion is impossible in the Connectivity Time model even in the presence of several other strong model assumptions. This further exhibits that the Connectivity Time model is indeed the weakest model among these three models. We believe other problems like exploration, gathering can be studied in our *T*-Path Connectivity model.
22.	PhishURLDetect: A parameter efficient fine-tuning of LLMs using LoRA for detection of phishing URLs **I Ali, B Subba** - ICDCN'25: Proceedings of the 26th International Conference on Distributed Computing and Networking, 2025 **Abstract:** This paper presents *PhishURLDetect*: a lightweight security framework for detecting phishing URLs based on fine-tuned Large Language Models (LLMs). It utilizes a proprietary corpus comprising 573,880 phishing and benign URLs to fine-tune two state-of-the-art LLMs, namely RoBERTa and GPT-2. Low-Rank Adaptation (LoRA) technique is employed to reduce the number of trainable parameters to 0.3% to 0.6% of the original LLM models without

	compromising on the performance. We demonstrate through experimental results that *PhishURLDetect* achieves high accuracy of 99.86%, and performs comparably to state-of-the-art LLMs while using significantly fewer number of trainable parameters.
23.	PLACO: A multi-stage framework for cost-effective performance in human-AI teams **PK Mallela, V Kumar, SS Jha, S Jain** - 27th European Conference on Artificial Intelligence (ECAI), 2024 **Abstract:** Human-AI teams have a pervasive impact in various fields including healthcare diagnosis, robotics in manufacturing, cyber-security, autonomous vehicles, and many more. The effectiveness of Human-AI teams highly depends on the set of humans that interact with the AI model for determining the final output. In this paper, we tackle the practical setting where taking the human input is of considerable cost and even expert humans can make mistakes. This paper proposes Probabilistic Labeler Assisted Cost Optimization (PLACO), a two-step framework to find cost-effective subsets of humans for multi-way classification tasks. The inputs from the subset of humans are then combined with the AI model's output resulting in the most accurate output. For cost-effective human selection given an input task, we estimate human labels by maximizing the posterior probability of a true human label given the AI model's output on the task. We further derive a value function that determines the value of a given human subset to maximize the lower bound on the overall accuracy of the Human-AI team. We present the theoretical foundations of our human label estimation method and human subset value function. We also empirically demonstrate the effectiveness of PLACO in terms of the Human-AI team's performance and cost-effectiveness against state-of-art methods on the CIFAR-10H and Imagenet-16H datasets having human annotations.
C	**Journal Article(s)**
24.	A comprehensive database for characterizing potential of common biomass feedstocks **SA Waziri, I Dhada, R Das** - Biomass Conversion and Biorefinery, 2025 **Abstract:** The escalating energy need caused by the global population expansion has compelled innumerable nations to alternate to sustainable and cleaner sources of energy for economic growth. Biomass as a sustainable energy source is often described through various metrics, predominantly by chemical composition, functional groups, calorific value, ash content, and other minor attributes. Moreover, these characteristics established from previous literature were found to be location-dependent. However, there is insufficient data to comprehensively evaluate commonly found biomasses of Indian origin and appraise their thermochemical potential. This study explores the energy and utility potentials of eight biomasses; poplar wood, eucalyptus wood, sugarcane bagasse, coconut shell, switchgrass, congress grass, rice husk, and corn cob through thermochemical characterization. Outcomes reveal that the feedstocks have high volatile matter (VM) of 74.3% ± 1.84% for eucalyptus, and 63.9% ± 0.5% for rice husk, the maximum high heating value (HHV) is 18.23 MJ/kg for poplar, and the minimum is 15.52 MJ/kg for congress plant. They also exhibit low moisture and ash content, which enhances combustion and prevents slagging. Attenuated total reflectance Fourier-transform infrared spectroscopy (ATR-FTIR)–based prominent peaks recorded are attributed to C-O, C-H, C = C, and O–H functional groups. Thermogravimetric analysis (TGA-DTG) demonstrated that maximum weight loss and major volatile gasses are released in the range of 220–411 °C ascribed to cellulose and hemicellulose, and decomposition of lignin happens at elevated temperatures. Pyrolysis–gas chromatography-mass spectrometry (Py-GCMS) shows several decomposition byproducts and pathways for the production of valuable industrial chemicals. Energy dispersive x-ray spectroscopy (EDX) and elemental mapping showed that the biomass mainly comprises carbon and oxygen.
25.	A novel approach to analyze the impact of groundwater drought on the perennial environment and hyporheic zone of surface water bodies

T Prashanth, S Ganguly, M Gummadi… - Journal of Hydrology, 2025

Abstract: Surface water bodies provide essential sources of fresh water for drinking, agriculture and industrial purposes. The hyporheic zone beneath and around surface water bodies plays a crucial role in maintaining the health and functionality of aquatic ecosystems. In recent times, surface water bodies have been observed to dry up rapidly in many parts of the globe due to groundwater drought. Hence, examining the sustenance of the surface water bodies over time is essential, which includes examining whether they are in a gaining or losing state and acting as perennial or non-perennial. In this context, this research aimed to analyze the behavioural changes in surface water bodies due to groundwater drought and stream-aquifer interaction in the Godavari Basin, India. This study proposes a new index called the Potential Stream-Aquifer Interaction Index (*PSAII*) or the Potential River Perenniality Index (*PRPI*) to define the nature of surface water bodies. This study employs satellite-derived bathymetry to determine water depth in ungauged lakes and Standardized Ground Water Table Index (*SGWTI*) to ascertain the magnitude of groundwater drought. The influence of groundwater drought on surface water bodies is determined based on the correlation of the head difference between groundwater table (GWT) and water surface elevation, as well as the *SGWTI*. The analysis reveals that *PRPI* for the upper Godavari River ranges from 0 to −0.4, and the lower Godavari River lies between 2.03 and 2.04 from 2009 to 2018, validated by the flow duration curves. The correlation between head difference and *SGWTI* lies between 0.8 and 0.9 for the upper Godavari and 0.08 to 0.48 for the lower Godavari River. The results imply that the upper Godavari river basin has become non-perennial due to groundwater drought. Based on the correlation analysis, it is also found that several ungauged lakes in the vicinity of the upper Godavari River are highly influenced by groundwater drought.

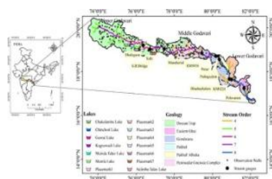

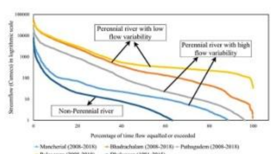

26.

[A Novel DC capacitor deficit power balancing mechanism for innate maximum power tracking with eliminated regulators in PV-inverters]

A Kumar, KR Sekhar - IEEE Transactions on Industrial Electronics, 2025

Abstract: In grid-connected inverters, dc capacitors maintain the dc bus voltage to feed the grid's regulated power. Nevertheless, the dc bus voltage influences the solar panel power extraction characteristics in a single-stage inverter configuration. Therefore, controlling the dc capacitor charge arbitrates solar energy extraction and simultaneous injection into the grid. At the initial start of the inverter, the dc capacitor is charged to the open circuit voltage of the solar farm, where the incoming power is zero but exhibits the maximum natural force for grid power injection. Allowing the grid power injection due to natural force alters the incoming solar power through an adaptive capacitor charge balance. By analyzing the natural phenomena of the exhibited forces on the dc capacitor during energy exchange, this work proposes a novel deficit power balancing model to derive the inverter modulation. The proposed power balancing mechanism eliminates the conventional power tracking algorithms, voltage, and current regulators while deriving inverter modulation. The derived inverter modulation through the proposed model naturally alters the inverter's operational equilibrium point to the maximum power point. Thus, regardless of irradiance, the system is stable at the solar farm's maximum

	power point. The efficacy of the proposed mechanism is verified on hardware.
27.	A pilot study on influence of natural rubber latex stabilization on swelling-consolidation behaviour of soil **U Veena, N James** - Indian Geotechnical Journal, 2025 **Abstract:** A few recent studies introduced natural rubber latex (NRL) as a stabilizer for improving the mechanical properties of soil such as ductility, compressive and tensile strengths, durability, etc. However, none of these studies addressed the effect of NRL treatment on swelling and compressibility of soil. The present study investigates the effect of NRL treatment on swelling and compressibility characteristics of three soils of different plasticities by conducting oedometer tests. Untreated and NRL-treated samples of the selected soils were prepared with the same soil dry density. For preparing treated samples, in place of water, NRL was added to soil. The results of one-dimensional swelling-compression tests demonstrated that in low and medium plastic soils, NRL treatment increased the swelling potential marginally, whereas it considerably reduced the swelling in the high plastic soil, which is expansive in nature. NRL did not cause any changes in the swelling pressure of medium plastic soil. At the same time, it brought about a considerable drop in the swelling pressure of high plastic soil. In the consolidation tests, a decrease in compressibility, quantified in terms of compression index, was observed in all soils after NRL treatment. The resilient nature of rubber content caused an increase in the recompression index in all treated samples. A reduction in the coefficient of consolidation was observed in NRL-treated soils. The study concludes that despite the high deformability of rubber, NRL treatment does not negatively affect the swell-compression behaviour of soils. Besides, the treatment effectively controls the swelling and compression of highly compressible soil.
28.	Additive strategies to mitigate humidity interference effects on PEDOT:PSS sensors for ammonia detection A Beniwal…**R Gond, B Rawat**, C Li - IEEE Sensors Journal, 2025 **Abstract:** Development of precise and accurate ammonia sensors suitable for healthcare (point-of-care devices) and environmental monitoring is imperative and absolute necessity. However, a persistent challenge in the gas sensor technology is sensitivity degradation due to humidity interference. To address this challenge, this study presents a screen-printed, flexible, and disposable sensor based on poly(3,4-ethylenedioxythiophene): poly(styrenesulfonate) (PEDOT:PSS) mixed with additives having reduced humidity interference tailored for ammonia (NH_3) gas detection. Polar solvents such as ethylene glycol (EG), dimethylformamide (DMF) and dimethyl sulfoxide (DMSO) are used as additives with the base material PEDOT:PSS. Enhanced hydrophobicity is confirmed via contact angle measurements. Current-voltage (I-V) characteristic assessments reveal a linear ohmic behaviour, emphasising the heightened conductivity of the samples with additives compared to the PEDOT:PSS sensor. When assessing the humidity response, the DMF modified PEDOT:PSS sensor exhibited minimal % response, registering only 37.01% at 90% humidity. This was a marked improvement over the pristine PEDOT:PSS sensor, which recorded 118.5% at the same humidity level, and outperformed other additive variants. Regarding ammonia detection, the PEDOT:PSS/DMF sensor demonstrated an experimental detection ability up to 0.1 ppm with 0.91 % response and outperformed the ammonia sensing ability of pristine PEDOT:PSS. Effect of relative humidity (~5 %RH to 80 %RH) on ammonia gas sensing performance of PEDOT:PSS/DMF sensor is also conducted and compared with pristine PEDOT:PSS. The increment in sensor conductivity with rising ammonia concentrations is theorized due to the charge transfer, where ammonia's lone pair of electrons interacts with the covalent backbone of PEDOT:PSS, suggesting a plausible sensing mechanism.
29.	Anisotropic response of bidirectionally ice-templated alumina/epoxy composites **SN Tiwari, V Kumar, PK Agnihotri** - International Journal of Applied Ceramic Technology, 2025

	Abstract: This work investigates the anisotropic response of nacre-like lamellar alumina/epoxy composites at low and high strain rates. Ice-templated alumina with long-range aligned porous lamellar structures is fabricated at 20 vol% of ceramic part using bidirectional freeze casting method. The obtained porous structures are infiltrated with epoxy to fabricate lamellar alumina/epoxy composites. The compressive tests are performed on scaffolds and composites at different orientations relative to the freezing direction. The testing results reveal that infiltration has increased the uniaxial compressive strength of the scaffold substantially. The compressive properties are higher when loaded along the freezing direction, and it decreases when it is loaded away from the freezing direction. The strength of the composites exhibited a strong dependency on the loading direction and strain rates.
30.	Assessment of shallow rocking foundation supporting RC shear wall frame structure: a numerical study **RM Kannan, P Haldar, N James** - Bulletin of Earthquake Engineering, 2025 **Abstract:** In recent years, researchers have taken advantage of the nonlinear characteristics of the underlying soil to mitigate the excessive seismic force demands on the superstructure under earthquake excitation. For this purpose, the conventionally designed foundation can be replaced with rocking foundation. This is achieved by under proportioning the shallow foundation. Although the mechanism of rocking foundations has been well documented, there remains a gap in developing a methodology for reduction of foundation sizes in multi storey Reinforced Concrete (RC) shear wall framed structure. Therefore, this study focuses on the seismic responses of a shallow foundations supporting a multistorey RC shear wall framed structure. The foundation for RC shear wall is proportioned by gradually reducing the earthquake load considered for the foundations to enhance the increased rocking effect and to mitigate seismic force demands. Thereafter, key parameters responsible for seismic behavior of sub-structure are being compared with conventionally designed foundation with increasing foundation rocking, by varying type of underlying soil and with increasing height. Seismic behavior obtained by implementing a series of nonlinear time history analyses indicates that the foundation rocking greatly influences the dynamic properties. With increasing degree of foundation rocking, natural fundamental period of the overall structure gets lengthened, with decreasing peak roof acceleration, thereby mitigating the peak base moment and base shear experienced at the shear wall compared to conventionally designed foundation. On the other hand, it is observed that there is an increase in roof displacement and shear wall settlement at the foundation level. It is found that the foundation of shear wall can be designed by considering 40%, 60% of earthquake loads for zone V and zone II structural designs, respectively without encountering excessive settlements. From the sensitivity analysis it is highlighted that the foundation size and design seismicity impact the base shear contribution ratios between shear wall and column members, fundamental natural period and foundation settlement.
31.	Biphenylene-graphene van der Waals bilayer heterostructure as an anode material for Li-ion batteries **N Duhan**, B Chakraborty, **TJD Kumar** - Journal of Energy Storage, 2025 **Abstract:** The quest to discover a top-tier electrode material for lithium-ion secondary batteries continues to advance for the past many decades in order to satisfy the surging power necessities. Pristine two-dimensional nanolayer electrodes often face challenges such as poor cycling efficiency, slow diffusion, and low lithium capacity. Fabricating heterostructure bilayers from different two-dimensional materials is a compelling approach to combine their inherent attributes while mitigating the individual drawbacks of each material. Current research work showcases a thorough investigation of the biphenylene-graphene (BPN/G) van der Waals bilayer heterostructure through first-principles calculations, aimed at evaluating its viability in the role of lithium-ion battery anode. The BPN/G bilayer exhibits robust energetic and thermal stability, coupled with excellent electronic and ionic conductivity. The binding energy of lithium for

	BPN/G bilayer is calculated to be −0.97 eV, illustrating a significant improvement over that of the individual monolayers. Lithium atoms preferentially adsorb into the interlayer region initially and later occupy the outer surfaces. The bilayer achieves saturation to reach its maximum lithium storage capacity of 956 $mAhg^{-1}$, surpassing that of pure graphene. The diffusion energy barrier for lithium migration along various pathways varies from 0.47 eV to 0.26 eV. The low barrier and high diffusivity of 3.9×10^{-5} cm2/s, points toward high lithium mobility and excellent cycling efficiency. The BPN/G bilayer provides a beneficial operating voltage of 0.51 V, signifying stable cycling performance and safe operation. The outcomes indicate a high lithium storage capability, remarkable conductivity, smooth lithium mobility, and efficient voltage profile, validating the BPN/G bilayer as an ideal negative electrode component for lithium-ion secondary batteries. 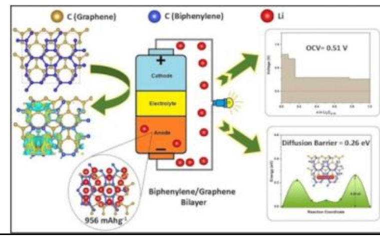
32.	BLE extended advertisements for energy efficient and reliable transfer of large sensor data in monitoring applications **S Gautam, S Kumar** - IEEE Transactions on Green Communications and Networking, 2024 **Abstract:** Advertising extensions introduced in Bluetooth Core Specification version 5.0 brought many feature enhancements like larger payload size, options for longer range, larger number of channels used, as compared to legacy advertisements introduced in version 4.0. Based on real-time energy consumption analysis, this paper deems BLE extended advertisements as the more energy-efficient choice as compared to legacy advertisements for applications with motion data generated at high sampling rates, and also highlights the range of data size for which legacy advertisements are more energy-efficient. For sensor networks using high data sampling rates, taking receiving link layer's behaviour into account, the paper analyses the merits and demerits of utilizing all 1650 bytes of an extended advertising event which is the maximum allowed limit. Extensive real-time experimentation carried out for varying amount of network congestion reveals that data loss mostly remains between 2-4% even in highly congested channel for large amount of data sent in each extended advertising event. However, because receiving link layer rejects partially received extended advertising events, sometimes, hiked losses are observed. Sending smaller data in each event yields more stable losses across the sensor network, but these losses are larger in higher network congestion, and energy efficiency is poorer. The paper highlights the potential and limitations of extended advertisements in applications under consideration, and emphasizes the need of the receiving link layer's capability to process partially received secondary channel packet chains.
33.	Bluetooth low energy-based novel power efficient buffalo calving detection solution **R Raina, KJ Singh, S Kumar**, S Jain - IEEE Networking Letters, 2025 **Abstract:** This letter focuses on tackling the challenge of accurately determining the timing of buffalo calving while prioritizing power efficiency. To achieve this, a novel, compact, lightweight and power efficient device is designed for buffalo comfort and can be conveniently attached to the tail. The device wirelessly transmits data to a gateway using Bluetooth Low Energy (BLE). This functionality becomes particularly crucial when the tail movement increases in the last 12 hrs before calving and is regarded as a key behavioral indicator for predicting the onset of labor. Moreover, when an accelerometer is tied to the buffalo's tail, the Z axis, which represents the vertical axis perpendicular to ground is anticipated to show the most notable deflections during this period as discussed in the literature. Thus, to conserve power, data is only

	transmitted when significant tail movement is detected, typically 12 hrs before calving i.e. when Mean Z > -3 m/s2. This approach reduces the device's power consumption, extending its battery life to more than 6.08 years (approx.) using 620 mAh / 3V battery.
34.	Boosted capacity and stability of aqueous iron-sulfur battery using DMSO as an electrolyte additive **M Singh, S Kaur, S Mehta, M Kumar, K Kumar, SK Meena, TC Nagaiah** - Energy Storage Materials, 2025 **Abstract:** Exploring metal-sulfur batteries with low cost, high safety, and capacity is the need of the hour for large storage applications. Iron (Fe) being a highly abundant and cost-effective element, provides an excellent option as an anode material which on coupling with abundant sulfur (S) in an aqueous electrolyte will be a game-changing approach. Despite a promising outlook, the stability of Fe anode due to side reactions in aqueous electrolytes and inherent corrosion tendencies limit their performance. Herein, we have explored dimethyl sulfoxide (DMSO) as an electrolyte additive in iron percholorate $(Fe(ClO_4)_2$ for aqueous Fe-S battery, which exhibited high specific capacity of 1145 mAh g^{-1} at 50 mA g^{-1} with remarkable cycling stability for 400 continuous cycles at 2.0 and 0.5 A g^{-1} current densities with 72 % and 98 % capacity retention respectively without replacing the Fe-anode. The addition of DMSO, suppressed parasitic hydrogen evolution reaction (HER) by 6.7 times and mitigated the corrosion rate of iron electrodes by 2.2 times as evidenced by the spectroscopic and gas chromatography techniques. The molecular dynamics (MD) simulations revealed that DMSO engages the water molecules through hydrogen bonding which reduced the fraction of free water molecules available for HER and corrosion of iron electrodes. 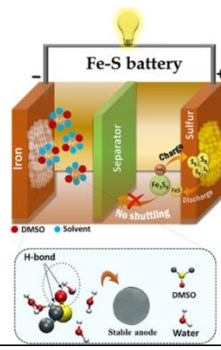
35.	Chemically modified Gelatin/Chitosan as a chemosensor adsorbent for detection of toxic metals and removal of organic dyes **A Singh, A Kumar**, N Kaur, **N Singh** - Polymers for Advanced Technologies, 2025 **Abstract:** Due to the vast amounts of toxic metals, oils, and dyes containing wastewater, water pollution is currently a serious health issue for human beings and animals. Adsorption of these pollutants using a biopolymeric-based hydrogel from wastewater is one of the potent methods due to its biodegradability and low cost. Herein, a porous and biodegradable hydrogel (CS–GL–IL) was synthesized from gelatin (GL), chitosan (CS), and ionic liquid (IL), acting as an excellent adsorbent for water pollutants. The maximum percentage swelling obtained for the synthesized CS–GL–IL hydrogel was 480% ± 3% for 0.5 g of the ionic liquid, 0.05 g of APS, and 35 mL of water at 65°C for 1.5 h of reaction. The process of eliminating methyl orange (MO) and methylene blue (MB) from a dye containing water was done using the CS–GL–IL hydrogel. Numerous methods, including PXRD, SEM, FTIR, and rheology, have been used for the characterization of the CS–GL–IL hydrogel. The obtained data indicate that the Freundlich adsorption isotherm with pseudo-second-order kinetics was followed for adsorption of dyes. The hydrogel exhibits excellent adsorption capacities of 1171 mg/g and 1062 mg/g for MO and MB, respectively. Furthermore, the hydrogel also exhibited efficiency in detection and adsorption of Ni2+ and Pb2+ with adsorption capacities of 315 mg/g and 370 mg/g, respectively. Dye removal

	efficiency remained above 82% even after eight iterations of dye adsorption and desorption experiments. Due to its high adsorption potential and regeneration capabilities, the CS–GL–IL hydrogel acts as an excellent material for remediation of wastewater.
36.	Compositional depths of cognitive semantics: Bridging perceptual experiences and conceptual structures K Pala, V Nedumpozhimana, **S Shalu** - Frontiers in Psychology, 2025 **Abstract:** The primary aim of this research was to investigate the intricate relationship between the structural elements of experiences and their essential role in meaning formation. The analysis focused on understanding the nature of mental representations and the subjective, phenomenal qualities that emerge within experiences. To achieve this, an integrated approach, combining cognitive semantics with phenomenological analysis, was employed to examine the compositional complexities of the dynamic interaction between a priori and immediate experiences and their significance in meaning formation. The study highlights the interconnectivity of structural elements within experience as a critical factor in shaping the phenomenal qualities of mental representations. Another key contribution of this study is the introduction of the “fulfiller” concept, which underscores the importance of absent qualities in meaning formation-an often-overlooked aspect in traditional models that focus solely on present attributes. The “fulfiller” concept emphasizes how absence, in addition to presence, influences meaning assignment. This inclusion enhances our understanding of meaning formation by considering both the tangible and intangible dimensions of the experiential-intentional process, offering a more comprehensive framework for understanding how meaning emerges from the complex interaction of present and absent qualities.
37.	Deep reinforcement learning based localization and tracking of intruder drone **S Kainth, SS Jha** - Journal of Computing and Information Science in Engineering, 2025 **Abstract:** Unmanned Aerial Vehicles (UAVs) are fast becoming a low-cost, affordable tool for various security and surveillance tasks. It has led to using UAVs (drones) for unlawful activities such as spying or infringing on restricted or private air spaces. Such rogue use of drone technology makes it challenging for security agencies to maintain the safety of many critical infrastructures. Additionally, due to the drones' varied low-cost design and agility, it has become challenging to identify and track them using conventional radar systems. This paper proposes a Deep Reinforcement Learning-based approach for identifying and tracking an intruder drone using a chaser drone. Our proposed solution employs computer vision techniques interleaved with a Deep Reinforcement Learning control for tracking the intruder drone within the chaser's field of view. The complete end-to-end system has been implemented using ROS and Gazebo, with an Ardupilot-based flight controller for flight stabilization and maneuverability. The proposed approach has been evaluated on multiple dynamic scenarios of intruders' trajectories and compared with a PID-based controller. The results show that the Deep Reinforcement Learning policy achieves a tracking accuracy of 85%. The intruder localization module is able to localize drones in 98.5 % of the frames. Furthermore, the learned policy can track the intruder even when there is a change in the speed or orientation of the intruder drone.
38.	Design flexible LuH_3 monolayer as an efficient water-splitting photocatalyst across a broad light spectrum XY Yang, **R Ahuja**, W Luo - Nano Energy, 2024 **Abstract:** Photocatalytic water splitting has attracted extensive attention for its bright prospects in producing clean hydrogen energy. To realize efficient solar-to-hydrogen energy conversion, it is important to explore a photocatalyst with high electron–hole separation and wide-range solar absorption. Herein, a novel two-dimensional metal-hydride, LuH_3, is designed and its viability as an efficient photocatalyst for overall water splitting is evaluated in the present work. It reveals that LuH_3 monolayer is an isotropic semiconductor with a direct band gap of 2.56 eV, decreased

	to 1.872 eV in a bilayer, exhibiting strong absorption efficiency for ultraviolet, visible, and near-infrared regions. Besides, it has favorable valence and conduction band positions for water redox reactions of O_2/H_2O and $H+/H_2$, high carrier mobility, and significant charge separation capability due to the orientation-dependent distribution in band edges, which play vital roles to enhance photocatalytic performance. The higher partial charge densities on H1b and H2d in HOMO lead to a more potent oxidation reaction, facilitating the reduction reaction and the production of hydrogen. In particular, LuH_3 monolayer is flexible and sensitive to external stress. Applying both isotropic and uniaxial strain has a limited impact on achieving favorable band alignments with water redox potentials, providing distinct opportunities for various applications. In both acidic and alkaline environments, LuH_3 monolayer shows significant potential for efficient photocatalysis in the context of overall water splitting. Furthermore, LuH3, a van der Waals material, can exfoliate from multilayered or bulk forms with a cleavage energy of 1.07 J/m^2, which is three times higher than the experimentally measured 0.37 J/m^2 for graphite. These findings highlight the potential of LuH_3 monolayer as an efficient solar-spectrum water-splitting photocatalyst, with implications for sustainable energy conversion technologies utilizing solar energy for clean and renewable hydrogen fuel generation. 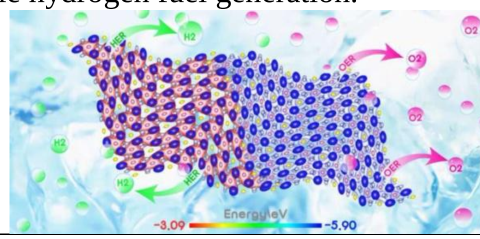
39.	DFT insights into bio-oil model oxygenates interaction on Co and Fe doped $LaNiO_3$ perovskite catalyst **A Goyal, PP Singh, A Banerjee, T Mondal** - Journal of the Indian Chemical Society, 2025 **Abstract:** Bio-oil steam reforming (SR) over metal oxides has emerged as a promising approach for hydrogen production. Perovskite (ABO_3) type metal oxides have shown exceptional performance in the SR process due to the synergistic effect of lanthanide materials at A-site and transition metals at the B-site in combined with the presence of oxygen vacancies that enhance their catalytic activity. Present study focuses on understanding these effects by investigating the adsorption energies of bio-oil model compounds, key intermediates and steam on the periodic slabs: $LaNiO_3$ (001), $LaNi_{0.8}Co_{0.2}O_3$ (001), and $LaNi_{0.8}Fe_{0.2}O_3$ (001), using density functional theory (DFT). The findings reveal that the synergistic effects of bimetallic catalysts cause significant variations in adsorption energies, which are influenced by molecular orientation and surface interactions, offering deeper insights into their catalytic behavior. Aromatic compounds like phenol, furfural, and benzaldehyde exhibit enhanced adsorption stability due to their unique interactions with the catalyst surface. The orientation of these compounds plays a crucial role in determining both strength and stability of their adsorption. Additionally, our observations indicate that CH species, due to their strong interaction with the catalyst, significantly contribute to carbon deposition on perovskite catalyst surfaces. Among the catalysts studied, $LaNi_{0.8}Fe_{0.2}O_3$ (001) exhibited the highest adsorption energy and the shortest bond lengths for bio-oil model compounds and steam, reflecting robust interactions. In contrast, $LaNi_{0.8}Co_{0.2}O_3$ (001) achieved the most optimum adsorption energies and bond lengths across all investigated molecules. The binding energy trend is: $LaNi_{0.8}Fe_{0.2}O_3$ (001) > $LaNi_{0.8}Co_{0.2}O_3$ (001) > $LaNiO_3$ (001). This study substantiates that the cobalt-doped $LaNiO_3$ (001) catalyst exhibits superior efficiency among the investigated perovskites, characterized by optimal molecular binding energies. These findings align with established experimental data, highlighting $LaNi_{0.8}Co_{0.2}O_3$ (001) as an effective catalyst for steam reforming and advancing the potential for sustainable hydrogen production.

<table>
<tr><td></td><td>
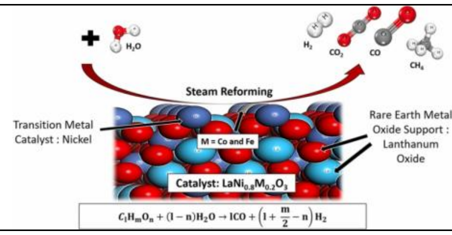

</td></tr>
<tr><td>40.</td><td>

[Disposable and highly sensitive humidity sensor based on PEDOT:PSS/GO heterostructure]

P Shukla, R Gond, A Beniwal, C Li, **B Rawat** - IEEE Journal on Flexible Electronics, 2025

Abstract: This work reports a flexible and disposable high-performance humidity sensor using the poly(3,4-ethylenedioxythiophene) polystyrene sulfonate (PEDOT:PSS) and graphene oxide (GO) heterostructure. The fabrication of the sensor is done using a cost-effective and large-scale production methodology, which involves the screen printing process for electrodes and spin-coating for sensing layer depositions. Contrary to the PEDOT:PSS, the heterostructure sensor exhibits enhanced humidity sensing performance with high response and quicker response time. At room temperature (RT), the sensor exhibits excellent sensitivity of around 3.953%/RH over a detection range from 10% RH to 60%RH. The device also possesses excellent repeatability, long-term stability, and robustness against temperature variations. These findings suggest that PEDOT:PSS/GO heterostructure holds great potential as an effective sensing material for high-performance humidity sensor development for agriculture, medical, and industrial applications.
</td></tr>
<tr><td>41.</td><td>

[Electrochemical ring opening and [3 + 2] cycloaddition of aziridines: Access to 1,2-bifunctionalized products and Imidazolines]

S Dutt, N Duhan, V Kale, P Banerjee - Organic Letters, 2025

Abstract: Herein, we report an electricity-driven activation of aziridine via direct anodic oxidation to give *N*-heterocycles and 1,2-bifunctionalized products by excluding any oxidant/reductant or metal catalyst. Many structurally modified aziridines were employed in the presence of different nitriles. A large variety of nucleophiles were screened to furnish chemoselectively O-alkylated and C-alkylated products. Late-stage derivatization of aziridine with natural and medicinally active compounds has also been done. Remarkably, our strategy was found to be a greener, sustainable, and atom-economical approach (*E*-factor = ca. 0.8). Azetidine was also found to be compatible with our protocol and generated six-membered *N*-heterocycles. The detailed mechanistic study highlighted that the reaction is driven via the generation of an aziridine radical cation followed by the S_N2 nucleophilic attack.

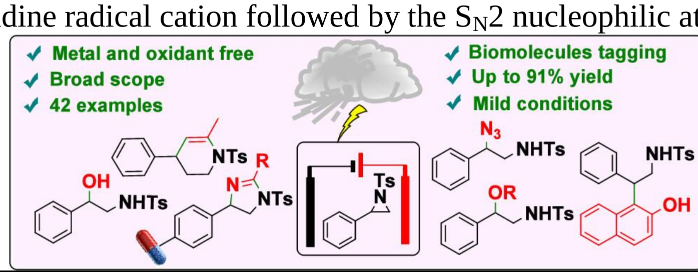

</td></tr>
<tr><td>42.</td><td>

[Electroredox N-heterocyclic carbene-catalyzed enantioselective (3 + 3) annulation of Enals with 2-Naphthols]

V Kale, S Shee, **S Dutt, N Sinha**, AT Biju, **P Banerjee** - Organic Letters, 2024

Abstract: Developing asymmetric transformations using electroredox and N-heterocyclic carbene (NHC)-catalyzed radical pathways is still desirable and challenging. Herein, we report an iodide-promoted β-carbon activation (LUMO-lowering process) of enals via electroredox carbene catalysis coupled with a hydrogen evolution reaction (HER). This strategy offers an environmentally friendly and sustainable route for rapidly assembling synthetically useful chiral naphthopyran-3-one in good to excellent yield and enantioselectivity using traceless electrons as inexpensive and greener oxidants. The mechanistic studies and cyclic voltammetry suggest that
</td></tr>
</table>

<table>
<tr><td></td><td>the reaction proceeds via direct single electron transfer (SET) of the in situ-generated Breslow intermediate.
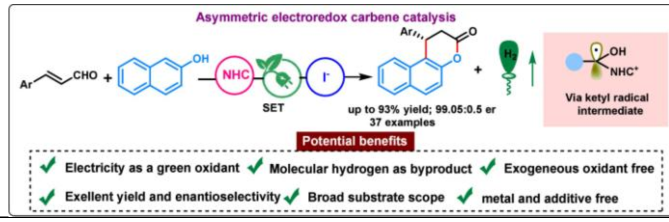
</td></tr>
<tr><td>43.</td><td>Energy-efficient concrete roofs for buildings: Integrating macroencapsulated nano-enhanced PCMs for hot climate adaptation
PJ Abass, S Muthulingam - Case Studies in Thermal Engineering, 2025

Abstract: Direct sunlight on concrete roofs raises interior heat flow and cooling demands. Latent heat storage with phase change materials (PCMs) offers passive cooling, but nanomaterials are needed to improve their low thermal conductivity. In this study, a two-way hollow concrete roof (HCR) integrated with macroencapsulated nano-enhanced PCM (NePCM) is developed for passive cooling and tested under ambient conditions. Characterization of selected organic PCM (OM35) is conducted individually and in combination with 2 % and 4 % mass fractions of multi-walled carbon nanotubes (MWCNT) and graphene nanoplatelets (GNP). Following unit cell approach, a conventional concrete roof (CCR) without PCM and three HCR specimens are cast: OM35–SU, 2%GNP–NePCM, and 4%GNP–NePCM. Thermal performance of the four specimens is assessed by analyzing temperature variations, heat flow, thermal load, decrement factor, and time lag. It is observed that thermal conductivity enhances 36.4 % and 45.5 % in 2 % and 4%GNP–NePCMs over OM35. During sunny hours, OM35–SU, 2 %, and 4%GNP–NePCMs reduce indoor surface temperatures by an average of 8.1, 8.7, and 9.6 °C, respectively. Cooling loads in 2 % and 4 % GNP–NePCMs are 68 % lower than CCR. Further, 2 % and 4 % GNP–NePCMs have 33 % and 36 % less mean time lag than OM35–SU. The findings offer valuable insights into the macroencapsulation of NePCM in roof slabs, enabling effective thermal energy management for indoor environments in hot climates.</td></tr>
<tr><td>44.</td><td>Enhancing performance of machine learning tasks on edge-cloud infrastructures: A cross-domain Internet of Things based framework
O Almurshed, **A Kaushal**, S Meshoul, A Muftah, O Almoghamis, I Petri, **N Auluck**, O Rana - Future Generation Computer Systems, 2025

Abstract: The Internet of Things (IoT) and Edge-Cloud Computing have been trending technologies over the past few years. In this work, we introduce the Enhanced Optimized-Greedy Nominator Heuristic (EO-GNH), a framework designed to optimize machine learning (ML) and artificial intelligence (AI) application placement in edge environments, aiming to improve Quality of Service (QoS). Developed specifically for sectors such as smart agriculture, industry, and healthcare, EO-GNH integrates asynchronous MapReduce and parallel meta-heuristics to effectively manage AI applications, focusing on execution performance, resource utilization, and infrastructure resilience. The framework carefully addresses the distribution challenges of AI applications, especially Service Function Chains (SFCs), in edge-cloud infrastructures. It contains Data Flow Management, which covers aspects of data storage and data privacy, and also considers factors like regional adaptations, mobile access, and AI model refinement. EO-GNH ensures high availability for forecasting, prediction, and training AI models, operating efficiently within a geo-distributed infrastructure. The proposed strategies within EO-GNH emphasize concurrent multi-node execution, enhancing AI application placement by improving execution time, dependability, and cost-effectiveness. The efficiency of EO-GNH is demonstrated through its impact on QoS in real-time resource management across three application domains, highlighting its adaptability and potential in diverse cross-domain IoT-based environments.</td></tr>
<tr><td>45.</td><td>Enhancing transparency in global horizontal irradiance estimation with tree based machine</td></tr>
</table>

	learning algorithms and Shapley additive explanations framework R Gupta, C Ganvir…**RK Baghel** - International Journal of Ambient Energy, 2025 **Abstract:** The estimation of global horizontal irradiance (GHI) is crucial for assessing solar energy potential, especially for investment purposes in specific regions. This study employs two feature selection techniques such as recursive feature elimination (RFE) and least absolute shrinkage and selection operator (LASSO) to identify key variables from two datasets, which are then used to train four machine learning (ML) models such as Decision Tree (DT), Random Forest (RF), Extreme Gradient Boost (XGB), and Extra Trees (ET) regressors. The performance of these models is evaluated using three statistical metrics such as mean absolute error (MAE), root mean squared error (RMSE), and *R*-squared (R^2). The results show that the ET regressor, when combined with LASSO, achieves the best predictive performance, with an MAE of 1.36 W/m^2 and an RMSE of 2.46 W/m^2. The study further employs Shapley Additive Explanations (SHAP) to interpret the model, revealing that parameters like Diffuse Horizontal Irradiance, Solar Zenith Angle, and Direct Normal Irradiance significantly impact GHI prediction accuracy. The combination of feature selection, advanced ML models, and SHAP analysis offers a comprehensive and transparent framework for solar energy resource assessment, addressing the need for accuracy and interpretability in GHI estimation.
46.	Ensemble deep generalized eigen-value random vector functional link network for classification problems **MA Ganaie, Y Kumar, A Bhatia, C Jayrajsinh** - Computers and Electrical Engineering, 2025 **Abstract:** Random vector functional link neural networks have been widely used across applications due to their universal approximation property. The standard random vector functional link neural network consists of a single hidden layer network, and hence, the generalization suffers due to poor representation of features. In this work, we propose ensemble deep generalized eigen value proximal random vector functional link (edGERVFL) network for classification problems. The proposed edGERVFL improves the architecture twofold: generating a better feature representation via deep framework, followed by the ensembling of the base learners, composed of multilayer architecture, to improve the generalization performance of the model. Unlike standard RVFL-based models, the weights are optimized by solving the generalized eigenvalue problem. To showcase the performance of the proposed edGERVFL model, experiments are conducted on diverse tabular UCI binary class datasets. The experimental findings, coupled with the statistical analysis, indicate that the edGERVFL model outperforms the provided baseline models. 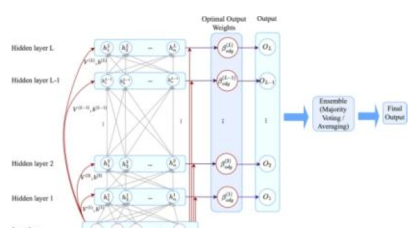
47.	Estimability analysis and optimization of soil hydraulic and abiotic stress parameters from root zone salt-water dynamics in soil column lysimeter **A Kumar, I Sonkar** - Plant and Soil, 2025 **Abstract:** Background and aims: Root water uptake (RWU) depends on root development, influenced by water and salt stress (WAS). Modeling RWU requires calibration of soil and root parameters using lysimeter data, which is challenging. The study introduces a global sensitivity index-based estimability method for parameter assessment and selection, optimizing them using observations from lysimeter experiments. Methods: A variance-based global sensitivity and estimability analyses was performed on the HYDRUS-1D model. The analyses evaluate the impact of soil hydraulic and stress parameters on pressure head, soil moisture, bottom flux, and

	electrical conductivity. Interactions among parameters across the root zone were analyzed for model parameter selection. The selected parameters were calibrated from soil-column lysimeter experiments on berseem (*Trifolium alexandrinum*) under saline and non-saline conditions. Results: The analyses identify water stress and residual soil moisture as less estimable, while major soil and salt stress parameters as more estimable, especially from bottom flux and soil moisture data. Excluding saturated soil moisture, which strongly influenced parameter estimability, improved optimization results. For the maximum scenarios, the simulated salt-water dynamics showed fair agreement with the observed data ($r^2 > 0.7$). For moderate salinity, reduced RWU was compensated by an increase of 0.01 d^{-1}, while high salinity significantly reduced this compensation to 0.002 d^{-1} with uniform RWU of 0.004 d^{-1}. Conclusion: The study demonstrates how different data sets contribute to accurate parameter estimation. Under high salinity, the compensation mechanism for reduced RWU was diminished, and the prolonged uniform RWU pattern suggested potential permanent root morphological changes.
48.	Exploring the potential of homologous epitopes from gut microbes for SARS-CoV-2 vaccine design, using molecular modelling to gain critical insights **S Prajapati, JA Malik, S Gupta, T Lamba, MA Zafar, MA Khan, S Nanda, Y Mehta, JN Agrewala** - Biologia, 2025 **Abstract:** This study addresses the role of gut microbiota in developing cross-reactive vaccines to protect against SARS-CoV-2. The gut microbiota positively influences lung diseases and is disrupted by respiratory infections. Exploring the interplay between gut microbes and SARS-CoV-2 is crucial. The gut is home to trillions of bacteria that release antigens that could cross-react with various pathogens. We aimed to identify T-cell and B-cell epitopes from gut microbiota and determine their potential cross-reactivity with SARS-CoV-2. We found that gut microbial species from *Gamma proteobacteria* and *Bacillus* classes show the highest similarity with SARS-CoV-2 proteins, suggesting these microbes are promising targets for epitope prediction and vaccine design. HLA-I and HLA-II epitopes demonstrated high promiscuity across multiple HLA alleles, enhancing their vaccine design potential. Immunogenicity assessments revealed that specific epitopes, like KITEHSWNA and QKALGGSVAIKITE, were highly immunogenic. The constructed vaccine exhibited stability, favorable physicochemical properties, and effective antigenicity. Structural validation, molecular docking, and molecular dynamics with TLR-4 confirmed the vaccine's potentials for immune activation. Immune simulations indicated robust immune responses, including significant IgM and IgG production and long-lasting memory B cells. This study highlights the potential of using cross-reactive epitopes from the gut microbiota to design effective vaccines, offering a promising strategy to enhance immune protection against SARS-CoV-2 and potentially other pathogens.
49.	Flexible inflation targeting and exchange rate passthrough in India: A Markov switching analysis **SA Shah** - Emerging Markets Finance and Trade, 2024 **Abstract:** This study investigates the exchange rate passthrough during the pre and post-inflationary targeting period. The study employs a regime-switching Markov approach to examine the dynamics of exchange rate and inflation in India. The findings provide that exchange rate passthrough follows a nonlinear pattern with high exchange rate variations bringing small changes in inflation and vice-versa. This contrasts with the existing literature, which confirms the linear relationship between the exchange rate and domestic prices. The nonlinear behavior of ERPT reflects that with changes in the exchange rate, domestic price levels are asymmetrically affected due to the kind of monetary policy in vogue. Further, the asymmetric behavior of exchange rate passthrough with a switching effect underscores the role of multitude of domestic and external factors that prevent the complete transmission of exchange rate changes to domestic inflation. The policy implications of the present study assert that to enhance exchange rate passthrough and to ensure the price parity in an inflationary targeting monetary policy regime, it is imperative to consider the role of the exchange rate in the monetary policy given its shock-

	absorbing feature.
50.	[Gamma-spectroscopic assessment of radionuclides and radiological hazards in undisturbed and cultivated soils of Rupnagar, Punjab, India] **SS Kaintura, S Devi, K Tiwari, S Thakur, R Sebastian, PP Singh** - Nuclear Engineering and Technology, 2025 **Abstract:** The current study provides a detailed comparison of radionuclides (^{238}U or ^{226}Ra, ^{232}Th, and ^{40}K) concentrations, elemental ratios, and radiological hazards in soil samples from undisturbed and cultivated lands in Rupnagar, Punjab, employing a high-purity germanium (HPGe) detector. The mean elemental concentration of ^{238}U, ^{232}Th, and ^{40}K in undisturbed land was found to be 4.70 ± 1.16 ppm, 20.63 ± 4.53 ppm, and 1.44 ± 0.15%, respectively, whereas, in cultivated land, the concentrations were 3.25 ± 0.28 ppm, 15.90 ± 0.96 ppm, and 1.92 ± 0.25%, respectively. Moreover, the elemental ratios ^{232}Th: ^{238}U, ^{232}Th: ^{40}K, and ^{238}U: ^{40}K have been established to assess the depletion or enrichment of radionuclides. Key radiological parameters, including the internal hazard index (Hin) and external hazard index (Hex), gamma index (Iγ), and alpha index (Iα), were found to be below the safe limit of unity . However, gamma dose metrics such as the absorbed dose rate (Ḋ), annual effective dose (AD), annual gonadal equivalent dose (AGED), and excess lifetime cancer risk (ELCR) considerably exceeded the global average. The relationship between radionuclide concentrations and health risk metrics was analyzed through their correlation. The morphology of soil particles from both sites was interpreted considering their radioactive properties.
51.	[Gelatin multiwalled carbon nanotube composite 3D printed semi biological mesh for abdominal hernia treatment] **P Yadav, A Mukherjee, JH Rajput, AP Choudhari, A Poundarik, B Das** - Chemistry–An Asian Journal, 2025 **Abstract:** Hernia is characterized by the protrusion of organs or tissue through weakened areas in the abdominal cavity wall. A common treatment for hernia involves the implantation of a mesh which promotes the growth of new tissue around or within the implanted material in the damaged area. The mesh is typically made from synthetic materials like polypropylene. However,such meshes has safety concerns like biofilm and scar tissue formation, foreign body reactions, and chronic pain. These concerns gave rise to development of biological meshes. Owing to mechanical weakness,biological meshes fail due to migration and rapid degradation . This study is aimed to develop a mechanically viable biopolymer-based composite degradable mesh. A gelatin-MWCNT composite 3D printed mesh has been developed with different pore sizes and filament sizes. Adding MWCNTs improved the composite's ductility, printability,hydrophilicity, modulus, and reduced its' degradation rate. The 3D-printed mesh also showed signs of cell attachment and proliferation representing non-toxicity of MWCNTs within the composite materials. The data showed improved cell adherence due to the incorporation of MWCNTs within the composite materials. Among the various material compositions tested, the composite material with gelatin with 0.01g MWCNTs gave the optimum mechanical strength and biocompatibility results.
52.	[Glacier area variation in Uttarakhand Himalaya: Investigating trends and influencing factors] **I Shrivas**, S Guha, **RK Tiwari**, M Prajapati, **AL Taral** - Earth Surface Processes and Landforms, 2025 **Abstract:** Understanding the intricate interplay between topography and glacier changes is vital for predicting future water resources and addressing the impacts of climate change. This study examines changes in glacier area in the Uttarakhand Himalayan region, where the River Ganga originates, between 2000 and 2023 using high-resolution satellite imagery. A manual digitization process was employed to delineate the glacier boundaries of 116 glaciers for the years 2000 and 2023. Multivariate regression analysis was then conducted to identify and quantify the

	controlling topographical and morphological parameters. The analysis revealed significant reductions in total glacier area, decreasing from $979.05 \pm 46.89\,km^2$ in 2000 to $957.60 \pm 13.67\,km^2$ in 2023, with an overall deglaciation rate of 0.095% per year, highlighting variability in glacier responses. This variability is driven by a complex interplay of mainly slope, shape index, glacier elevation and surface ice velocity. Among these factors, the shape index emerged as the most influential. Glaciers with a higher shape index (more elongated) were found to be more stable than those with a lower shape index (more circular). A 10% difference in shape index results in a glacier with a higher shape index losing 0.112% per year less area compared to a glacier with a lower shape index. The second controlling parameter is glacier slope; glaciers with a 10% steeper slope lost 0.11% per year less area compared to those with a gentler slope. The other two parameters showed some minor impact on glacier area variation in the sample glaciers but not across the entire Uttarakhand region.
53.	Graphene oxide/ polylactic acid composites with enhanced electrical and mechanical properties for 3D-printing materials A Pandey, J Singh, **M Singh**… - Journal of Molecular Structure, 2025 **Abstract:** Polymeric materials have gained significant attention as a captivating class of materials in the realm of additive manufacturing. Nevertheless, their extensive use remains constrained due to inherent limitations of low mechanical strength, thermal and electrical properties. Consequently, polymer composites are attaining consideration of the researchers for the development of customized materials with specific applications. In the present work, graphene oxide (GO) was synthesized using pencil lead as a precursor via modified Hummer's method and used for the fabrication of GO-based polylactic acid (PLA) composites with GO concentration variation from 0.25 wt% to 1.25 wt% with a step size of 0.25. The molecular conformation and characteristics of synthesized GO were analysed by X-ray diffraction (XRD), Energy dispersive X-ray spectroscopy (EDX), Raman spectroscopy, and Fourier transform infrared spectroscopy (FTIR). For mechanical and electrical properties evaluations, the required specimens were fabricated by direct ink writing through syringe extrusion method. It was observed that the 0.5 wt% loading graphene oxide showed the maximum value of tensile strength; however, 1.25 wt% GO content resulted in highest young's modulus. In contrast, at 1.25 wt% GO loading, compressive strength and microhardness exhibited the highest value among all the composites. The highest value of electrical conductivity of 58.91 μS/m was observed at 1.25 wt% GO content. However, maximum dielectric constant value of 307.69 was obtained at 1 wt% GO loading at100 Hz frequency. Thus, in our findings, the inclusion of a small amount of GO in PLA matrix enhanced the mechanical as well as electrical properties.
54.	Graphene–nickel oxide–polyaniline ternary nanocomposite-embedded epoxy coating on mild steel for corrosion protection R Saini, RN Goswami… **Kumar, N Kumar**… - Advanced Engineering Materials, 2025 **Abstract:** The present work addresses the synthesis and application of graphene-based ternary nanocomposite for anticorrosion performance to protect mild steel in an accelerated corrosive environment. The chemically-functionalized graphene-nickel oxide (Gr-NiO)-PANI ternary nanocomposite is synthesized by the hydrothermal reduction of graphene oxide (GO) and nickel salt in the presence of urea, followed by interfacial wrapping of Gr-NiO by in situ grown polyaniline (PANI). The transmission electron microscopic images reveal the wrapping of Gr-NiO by PANI in the Gr-NiO-PANI ternary nanocomposite. The spectroscopic analyses (Fourier transform infrared and Raman) suggest the multiple interactions between Gr-NiO and interfacially grown PANI in Gr-NiO-PANI. The thoroughly blended Gr-NiO-PANI ternary nanocomposite into epoxy matrix via interfacial interactions provides uniform coating (thickness: $87 \pm 6\,\mu m$) on mild steel and increases the hardness by 160%. The corrosion inhibition performance of PANI, Gr-PANI, and Gr-NiO-PANI nanocomposites in epoxy coating is probed based on electrochemical and salt spray measurements in a 3.5% NaCl solution. The Gr-NiO-

<table>
<tr><td></td><td>PANI in the epoxy coating substantially enhances the total impedance and protects the underneath mild steel. The salt spray tests further corroborate the electrochemical results and demonstrate substantial enhancement in corrosion inhibition by Gr-NiO-PANI nanocomposite with no sign of corrosion even after 10 days, revealing its potential to mitigate corrosion of mild steel-based structural and engineering installations.</td></tr>
<tr><td>55.</td><td>

High performance ozone nanobubbles based advanced oxidation processes (AOPs) for degradation of organic pollutants under high pollutant loading

P Koundle, **N Nirmalkar**, G Boczkaj - Journal of Environmental Management, 2025

Abstract: Advanced Oxidation Processes (AOPs) have proven to be an effective solution for chemical wastewater treatment, particularly for degradation of organic pollutants, especially dyes. Ozonation is recognized as one of the most prevalent AOPs. Nevertheless, some cases show a lowered efficiency of O_3 utilization which is attributed to its inadequate distribution in the treated water causing low residence time, low mass transfer coefficient as well as shorter half-life. This study demonstrates the application of ozone nanobubbles to enhance the degradation of organics under high pollution load conditions. We propose an integrated method that utilizes bulk nanobubbles to enhance the reactivity of ozone for the degradation of organics. We examined the degradation of organic pollutants under parameters such as varying pH levels, ozone concentrations and presence of salts and surfactants. The degradation of the organic pollutant by ozone nanobubbles (0.177 L $mg^{-1}min^{-1}$) demonstrated a threefold increase in reaction rate constants compared to microbubbles (0.025 L $mg^{-1}min^{-1}$). The plausible reason for these findings is (i) higher mass transfer coefficient (ii) higher ozone solubility (iii) NBs may act as a surface for chemical reaction (iv) NBs may increase the half-life of ozone. The presence of reactive oxygen species was verified using scavenging tests. This part of the studies revealed contribution of reactive oxygen species (ROSs) such as hydroxyl radical ($^{\bullet}OH$), superoxide radical anion ($O_2^{\bullet -}$) and singlet oxygen ($^1O_2$) in the degradation process. The conditions that provide total degradation of 100% in 300 s for both organic pollutants (Green rit and methylene blue dye) are: 5 LPM (Litre per minute) ozone flow rate, acidic pH, monovalent salts (NaCl, 2 mM) and lower concentration of surfactants (CTAB and SDS, 0.3 CMC). A degradation mechanism has been outlined based on intermediates identified by LC-MS. This work presents a new method that combines AOPs with nanobubbles, which should lead to increased environmental sustainability and efficiency.

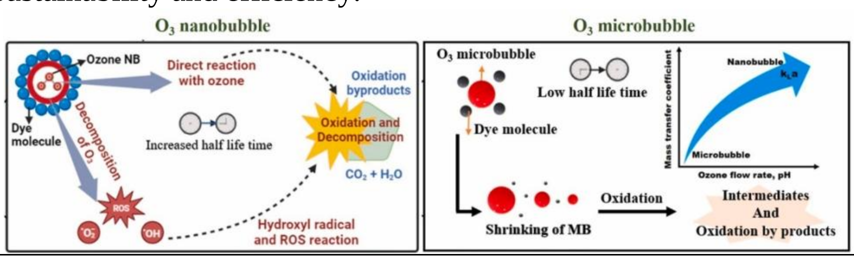

</td></tr>
<tr><td>56.</td><td>

Hybrid FR-AHP approach for GLOF hazard assessment in the Himalayan region

D Gaikwad, A Tyagi, **RK Tiwari** - Remote Sensing Applications: Society and Environment, 2024

Abstract: Glacial lakes in the Himalayan region have triggered numerous glacial lake outburst floods (GLOFs), leading to extreme flash floods and extensive destruction. Therefore, identifying hazardous glacial lakes is essential for sustainable development and protecting downstream populations. This study focuses on GLOF susceptibility mapping (GLOFSM) of glacial lakes by combining the analytical hierarchy process (AHP) and frequency ratio (FR) methods across the entire Himalayan region. The hybrid FR-AHP model reduces the number of subjective opinions and incorporate data-driven knowledge, hence, enhancing the accuracy of the GLOFSM. Based on 25 historical GLOF events, this method assigns weights to twelve selected factors and their subclasses, including lake area, glacier area, mean slope of the lake, mean slope of the glacier,

</td></tr>
</table>

	lake aspect, elevation, average SLA angle, dam height, avalanche risk, lake–glacier distance, precipitation, and temperature. The results revealed that the size of the lake has the greatest influence on the GLOFSM, followed by glacier size and dam height. In addition, of the 851 mapped glacial lakes, 324 were classified as highly hazardous, and 50 were classified as very highly hazardous in the region. Finally, we verified the accuracy of the generated GLOF susceptibility map via the area under the curve (AUC) model, which yielded a remarkable accuracy of 86.65%. Overall, these studies encourage the regular monitoring of hazardous glacial lakes and the planning of effective mitigation strategies to reduce the risk of glaciated river basins.
57.	In-beam γ-spectroscopy of ^{217}Ac D Sahoo, AY Deo, Madhu, **K Yadav**, SS Tiwary, PC Srivastava, R Palit, SK Tandel, A Kumar, P Dey, B Das, V Malik , A Kundu , A Sindhu, SV Jadhav, BS Naidu, AV Thomas - Physical Review C, 2025 **Abstract:** High-spin states in ^{217}Ac are reported up to 3.9-MeV excitation energy and $I^{\pi}=41/2^{+}$ where 22 transitions are newly observed. The structure of the yrast and near-yrast states below the $29/2^{+}$ isomer is revisited. The level structure above the $29/2^{+}$ isomer is established with firm spin and parity assignments. Large-basis shell-model calculations with the Kuo-Herling particle effective interaction are performed to compare the experimentally observed level energies with the theoretical predictions. A comparison with the systematics of the N=128 isotones suggests that the yrast structures result from a weak coupling of the odd proton to the even-even ^{216}Ra core, which is consistent with the shell-model configurations.
58.	Introducing regioselective disulfide linkages in peptides under pseudodilute conditions by harnessing brønsted acid-activated *N*-chlorosuccinimide **NM Tripathi, BK Das, A Chowdhury, V Gour, A Bandyopadhyay** - JACS Au, 2025 **Abstract:** Methods that assemble multiple peptide disulfide bonds in the solid phase (pseudodilute conditions) are in high demand for synthesizing disulfide-rich peptides. Yet, the existing repertoire of disulfide-forming orthogonal chemistries in the solid phase is often hindered by additional steps for protecting group removals as well as the absolute necessity of rare, customized orthogonal cysteine (Cys) building blocks. We now describe a conceptually new while operationally simple on-resin method for disulfide assembly with widely accessible Cys protecting groups (Trt, Acm, and ^{t}Bu) using acid-activated N-chlorosuccinimide (NCS) in a single step. In the process, S-^{t}Bu Cys emerged as a new orthogonal building block for the single-step assembly of the peptide disulfide. In our investigations, 2% TFA-activated NCS offered rapid (∼15 min) and a clean disulfide product in various peptides. Eventually, this novel strategy (2% TFA-NCS) was strategically merged in stepwise cross-linking with our previously described $I_2/S_2O_8^{2-}$-mediated disulfide assembly protocol to leverage two regioselective disulfide bonds into conotoxin, gomesin, and a de novo sequence within ∼30 min. Invariably, this new method proved highly productive and operationally simple. DFT calculations also support the hypothesis of NCS activation that assists efficient disulfide assembly in crossing a low-lying energy barrier via sulfonium intermediates. This newly developed method for ^{t}Bu deprotection and concomitant disulfide assembly in the solid phase should find wide applications in de novo peptide disulfide synthesis.
59.	Investigation of microstructural evolution and carbon redistribution in ausformed nanostructured

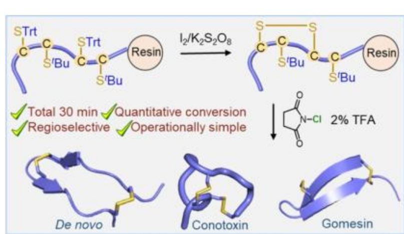

	bainitic steel via 3D atom probe tomography and its structure-property relationship **A Verma**, S Reza, S Ghosh, N Macha, **K Rakha** - Materialia, 2025 **Abstract:** Thermomechanical treatment is an important method to refine the microstructure and accelerate the kinetics of phase transformations in steels. In this study, different ausforming strains as 7 %, 15 %, 30 %, and 60 % were used to ausform steel samples at 570 °C temperature followed by isothermal holding at 350 °C for 10 days. X-ray diffraction was used to analyse the different phases present after thermomechanical treatment. Long isothermal holding for 10 days was used to develop a fully nanostructured bainitic microstructure consisting of bainitic ferrite and retained austenite films. Refinement of bainitic laths was observed with an increase in deformation strain. Atom probe tomography was further employed to study the carbon redistribution in the form of solid solution, clusters, segregation, and precipitation in a sample ausformed at 570 °C with 7 % strain. Atomic clustering was observed and quantified for the first time inside bainitic ferrite laths in nanostructured bainite, due to the dislocation substructure formed inside austenite as a result of ausforming. The maximum carbon content found in nano-scale particles was found to be 14.13 atomic % establishing the presence of clusters. The effect of ausforming on microstructural evolution, austenite stabilization, and carbon redistribution has been presented systematically in this work. 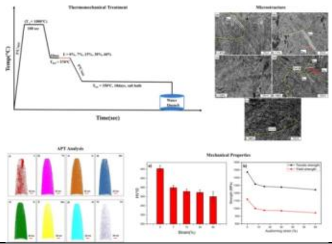
60.	Isolated neutral organic radical unveiled solvent-radical interaction in highly reducing photocatalysis **AC Shaikh**, MM Hossain, J Moutet… - Angewandte Chemie, 2025 **Abstract:** Diffusion-limited kinetics is a key mechanistic debate when consecutive photoelectron transfer (conPET) is discussed in photoredox catalysis. In situ generated organic photoactive radicals can access catalytic systems as reducing as alkaline metals that can activate remarkably stable bonds. However, in many cases, the extremely short-lived transient nature of these doublet state open-shell species has led to debatable mechanistic studies, hindering adoption and development. Herein, we document the use of an isolated and stable neutral organic ^{n}PrDMQA radical as a highly photoreducing species. The isolated radical offers a unique platform to investigate the mechanism behind the photocatalytic activity of organic photocatalyst radicals. The involvement of reduced solvent is observed, formed by single electron transfer (SET) between the short-lived excited state ^{n}PrDMQA radical and the solvent. In our detailed mechanistic studies, spectroscopic and chemical affirmation of solvent reduction is strongly evident. Reduction of aryl halides, including difluoroarenes is presented as a model study of the conPET method. Further, the activation of N_2O, a greenhouse gas that is yet to be activated by photoredox catalysis, is showcased in the absence of a transition metal. 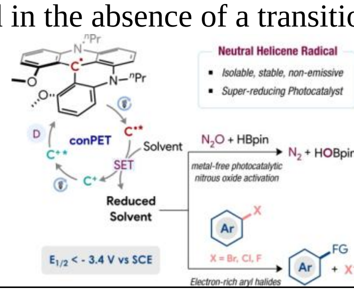
61.	Local resetting in a dynamically disordered exclusion process **N Bhatia, AK Gupta** - Physica A: Statistical Mechanics and its Applications, 2025

	Abstract: Inspired by the recycling process and obstruction faced by mRNA polymerase during gene transcription, we study an open, dynamically disordered, totally asymmetric simple exclusion process where particles all over the lattice locally reset to the entry site. The mean-field approximations have been employed to obtain analytical stationary-state characteristics such as density profiles, current, and phase boundaries. These results are validated by performing extensive numerical simulations. The role of hindrance-causing parameters is consolidated into a unifying parameter called the obstruction factor. The phase diagrams obtained for various choices regarding the resetting rate and the obstruction factor possess five stationary phases: three pure and two co-existing phases. Both the co-existing phases exist in a region and have localized domain walls. The quadruple and triple points in the phase diagram shift anti-diagonally with an increase in the resetting rate or the obstruction factor, expanding the region comprising the maximal-current phase. Further, potential phase transitions and the domain wall's behavior under the influence of resetting rates and the obstruction factor have been examined. The finite-size effect has also been scrutinized on the system's stationary-state characteristics.
62.	Machine learning models based on FEM simulation of hoop mode vibrations to enable ultrasonic cuffless measurement of blood pressure R Kumar, **V Kumar**…**Balendra**…**AK Sahani** - Medical & Biological Engineering & Computing, 2025 **Abstract:** Blood pressure (BP) is one of the vital physiological parameters, and its measurement is done routinely for almost all patients who visit hospitals. Cuffless BP measurement has been of great research interest over the last few years. In this paper, we aim to establish a method for cuffless measurement of BP using ultrasound. In this method, the arterial wall is pushed with an acoustic radiation force impulse (ARFI). After the completion of the ARFI pulse, the artery undergoes impulsive unloading which stimulates a hoop mode vibration. We designed two machine learning (ML) models which make it possible to estimate the internal pressure of the artery using ultrasonically measurable parameters. To generate the training data for the ML models, we did extensive finite element method (FEM) eigen frequency simulations for different tubes under pressure by sweeping through a range of values for inner lumen diameter (ILD), tube density (TD), elastic modulus, internal pressure (IP), tube length, and Poisson's ratio. Through image processing applied on images of different eigen modes supported for each simulated case, we identified its hoop mode frequency (HMF). Two different ML models were designed based on the simulated data. One is a four-parameter model (FPM) that takes tube thickness (TT), TD, ILD, and HMF as the inputs and gives out IP as output. Second is a three-parameter model (TPM) that takes TT, ILD, and HMF as inputs and IP as output. The accuracy of these models was assessed using simulated data, and their performance was confirmed through experimental verification on two arterial phantoms across a range of pressure values. The first prediction model (FPM) exhibited a mean absolute percentage error (MAPE) of 5.63% for the simulated data and 3.68% for the experimental data. The second prediction model (TPM) demonstrated a MAPE of 6.5% for simulated data and 8.73% for experimental data. We were able to create machine learning models that can measure pressure within an elastic tube through ultrasonically measurable parameters and verified their performance to be adequate for BP measurement applications. This work establishes a pathway for cuffless, continuous, real-time, and non-invasive measurement of BP using ultrasound.

	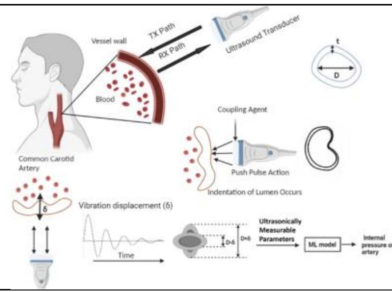
63.	[Mitigation of structural response on a floating elastic plate in the presence of multiple porous structures]() **G Sahoo**, V Venkateswarlu, **SC Martha** - Applied Ocean Research, 2025 **Abstract:** This study introduces a model comprising a series of porous structures of finite thickness positioned at a specific distance to secure the elastic plate (EP) for two cases (i) EP with free edges and (ii) EP with fixed edges from the incident waves. The porous structures are present on the seabed with finite gap regions to create the gap resonance. The study develops a system of equations by formulating the governing equation and considering boundary conditions under the framework of potential flow theory. These equations are then solved to analyze various factors, including plate deflection, shear force, strain of EP, and reflection, transmission, and dissipation coefficients. The investigation highlights the importance of breakwater structural parameters, such as length, porosity, and frictional coefficient, in mitigating plate deflection, shear force, and strain on EP. Moreover, the study identifies periodic harmonic oscillations in hydrodynamic coefficients, particularly affected by variations in the distance between structures. A configuration with four porous structures is highlighted for its exceptional wave-damping capacity, achieving nearly 65%. Furthermore, a comparative analysis reveals the superior wave-damping capability of setups incorporating four porous structures and EP compared to those with one, two and three porous structures installations. The differences in shear force as well as strain are presented for various combinations of porous structures and EP and compared with EP alone. Moreover, the plate deflection is greater and the reflection coefficient is lower for EP with free edges when compared to EP with fixed edges. As the mooring stiffness constant increases, the plate deflection decreases and the reflection coefficient increases. These findings hold significance for advancing the development of floating structures capable of withstanding severe wave conditions and minimizing shore-proximate wave impacts.
64.	[Morphine's role in macrophage polarization: Exploring M1 and M2 dynamics and disease susceptibility]() **JA Malik, JN Agrewala** - Journal of Neuroimmunology, 2025 **Abstract:** Morphine is a globally prevalent substance of misuse, renowned for its immunosuppressive effects mediated through opioid receptors expressed on immune cells. Macrophages are crucial antigen-presenting cells that fulfill diverse roles, such as antigen presentation, phagocytosis, wound healing, and disease protection. They are typically classified based on their activation states: M1 (proinflammatory), M2 (anti-inflammatory), and M0 (resting). Morphine significantly modulates immune responses and neuroinflammation, further complicating the landscape of opioid dependency and disease susceptibility. The association of macrophages under the influence of morphine needs to be understood under various diseased conditions. Several studies have been focused on investigating the impact of morphine on macrophage function and its implications in infectious diseases and brain-associated diseases. To light this subject, we have discussed recent advancements in understanding the influences between morphine, macrophage function, polarization, infection, brain tumors, and drug dependency. This article explores the complex relationship between morphine, macrophages, and related pathologies. Consequently, discussing deeper insights into these dynamics could guide effective treatments for substance abuse disorders.

65.	NCDT-CSS: Enhancing performance using non-coherent distributed transmission of chirp spread spectrum **A Gupta, S Agarwal** - IEEE Internet of Things Journal, 2025 **Abstract:** Internet-of-things (IoT) communication in rural areas faces significant challenges due to limited infrastructure and power constraints, making long-range communication difficult. To address this, we propose a novel non-coherent distributed transmission of chirp spread spectrum (NCDT-CSS) waveform that enables power-efficient, long-range communication by allowing multiple asynchronous transmitters to send the same data. Unlike existing methods, our NCDT-CSS framework uses a least-squares (LS)–based detector to extract symbols from the complex received signal without relying on intricate synchronization algorithms. The process involves estimating time, frequency, phase offsets, and channel conditions, followed by symbol detection using single-window (SW) and two-window (TW) LS-based detectors. Simulation results show that the NCDT-CSS framework, combined with an LS-based detector, offers superior bit error rate (BER) performance, contributing to an extended communication range. Additionally, hardware implementation validates the model's effectiveness, demonstrating enhanced data rates at a lower spreading factor (SF). These results confirm that the NCDT-CSS system is a robust solution for IoT communication in rural areas, providing low-power long-range capabilities with enhanced data rates.
66.	Noble-metal-free ZnII-anchored pyrene-based covalent organic framework (COF) for photocatalytic fixation of CO2 from dilute gas into bioactive 2-oxazolidinones **R Kishan, P Rani, N Duhan, TJD Kumar, CM Nagaraja** – ChemSusChem, 2025 **Abstract:** Photocatalytic conversion of CO2 into value-added chemicals offers a propitious alternative to traditional thermal methods, contributing to environmental remediation and energy sustainability. In this respect, covalent organic frameworks (COFs), are crystalline porous materials showcasing remarkable efficacy in CO2 fixation facilitated by visible light owing to their excellent photochemical properties. Herein, we employed Lewis acidic Zn(II) anchored pyrene-based COF (Zn(II)@Pybp-COF) to facilitate the photocatalytic CO2 utilization and transformation to 2-oxazolidinones. Notably, Zn-COF displayed absorption of visible light, with an optimal band gap of 1.8 eV, effectively catalyzing light-mediated functionalization of propargylic amines to 2-oxazolidinones under green conditions. Detailed experimental and theoretical mechanistic investigations demonstrated that light plays a crucial role in enhancing the efficacy of the photocatalyst, as it activates inert CO2 molecule to radical anion and thereby, lowers the energy barrier for its subsequent cyclization reaction with propargylic amine. Additionally, Zn-COF demonstrates promising catalytic performance utilizing dilute gas as the CO2 source. This is the first report regarding noble metal-free, Zn-COF exhibiting excellent photocatalytic carboxylative cyclization of CO2 with propargyl amines to prepare 2-oxazolidinones using dilute gas (13% CO2). This study offers a new direction for rationally constructing noble metal-free eco-friendly photocatalysts for achieving CO2 fixation reactions under eco-friendly conditions.
67.	Numerical simulation of effects of phase separation on viscous fingering in radial Hele-Shaw flows YF Deki, RX Suzuki…**M Mishra**… - Journal of Fluid Mechanics, 2025 **Abstract:** The Hele-Shaw–Cahn–Hilliard model, coupled with phase separation, is numerically simulated to demonstrate the formation of anomalous fingering patterns in a radial displacement of a partially miscible binary-fluid system. The composition of injected fluid is set to be less viscous than the displaced fluid and within the spinodal or metastable phase-separated region, in which the second derivative of the free energy is negative or positive, respectively. Because of phase separation, concentration evolves non-monotonically between the injected and displaced fluids. The simulations reveal four areas of the concentration distribution between the fluids: the

	inner core; the low-concentration grooves/high-concentration ridges; the isolated fluid fragments or droplets; the mixing zone. The grooves/ridges and the fragments/droplets, which are the unique features of phase separation, form in the spinodal and metastable regions. Four typical types of patterns are categorized: core separation (CS); fingering separation (FS); separation fingering (SF); lollipop fingering, in the order of the dominance of phase separation, respectively. For the patterns of CS and FS, isolated fluid fragments or droplets around the inner core are the main features. Fingering formation is better maintained with droplets in the SF pattern if the phase separation is relatively weaker than viscous fingering (VF). Even continuous fingers are well preserved in the case of dominant VF; phase separation results in lollipop-shaped fingers. The evolving trend of the patterns is in line with the experiments. These patterns are summarized in a pattern diagram, mainly by the magnitude of the second derivative of the free energy profile. 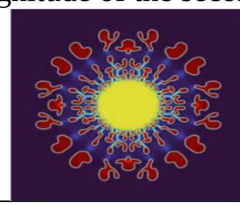
68.	On the inversion of generalized V-line transform of a vector field in $\mathbb{R}^2$ **R Bhardwaj**, RK Mishra, **M Vashisth** - Mathematical Methods in the Applied Sciences, 2025 **Abstract:** This article studies the inverse problem of recovering a vector field supported in $\mathbb{D}_R$, the disk of radius R centered at the origin, through a set of generalized broken ray/V-line transforms, namely, longitudinal and transverse V-line transforms. Geometrically, we work with broken lines that start from the boundary of a disk and break at a fixed angle after traveling a distance along the diameter. We derive two inversion formulas to recover a vector field in $\mathbb{R}^2$ from the knowledge of its longitudinal and transverse V-line transforms over two different subsets of aforementioned broken lines in $\mathbb{R}^2$.
69.	Rational design of porous organic framework (POF) for efficient conversion of CO2 to cyclic carbonates and 2-oxazolidinones at atmospheric pressure conditions **V Parihar, B Kumar, G Singh, CM Nagaraja** - Chemistry–An Asian Journal, 2025 **Abstract:** Carbon dioxide (CO_2) capture and its subsequent catalytic fixation into usable compounds represent a potential approach for addressing the energy problem and the implications of global warming. Hence, it is necessary to develop effective catalytic systems required for the transformation of CO_2 into valuable chemicals/fuels. Herein, we rationally designed a hydroxyl-functionalized porous organic framework (OH-POF) consisting of both acidic (OH) as well as basic N sites for the transformation of CO_2 using epoxides for the production of cyclic carbonates (CCs), a useful commodity chemical under environmental-friendly, metal/solvent/co-catalyst-free conditions. Moreover, OH-POF was post-synthetically modified to anchor non-noble metal, Zn(II) to generate Zn-POF and further explored it for the efficient functionalization of CO_2 with propargylic amines to generate valuable bioactive 2-oxazolidinones. Significantly, both OH-POF and Zn-POF demonstrated exceptional reusability with catalytic efficacy retained across numerous cycles of use. Notably, this study showcases a green and sustainable process for utilization of CO_2 under environmentally favorable ambient conditions into two highly valuable compounds, viz cyclic carbonates and 2-oxazolidinones.
70.	Recent breakthroughs in ring-opening annulation reactions of aziridines DR Mishra, **NP Mishra** - Organic & Biomolecular Chemistry, 2025 **Abstract:** Aziridines, characterized by their highly constrained three-membered nitrogen-containing heterocyclic ring system, serve as compelling synthetic intermediates for synthesizing numerous naturally occurring alkaloids and pharmaceuticals. The distinct ring strain arising from the geometric constraints of these sp3-rich trigonal rings imparts high reactivity, thereby offering

	a wealth of intriguing synthetic opportunities. Recent advances in the chemistry and reactivity of aziridines have unveiled significant progress in preparing more complex heterocycles. This review consolidates and examines recent publications on the ring-opening annulation reactions of aziridines, highlighting the latest breakthroughs, emerging trends, and future directions in this dynamic field.
71.	Red-light mediated formylation of indoles using a helical carbenium ion as a photoredox catalyst **AC Shaikh, N Lal, P Singh, Deepshikha** - Chemical Communications, 2025 **Abstract:** Low-energy photoredox catalysis has gained significant attention in developing organic transformations due to its ability to achieve high penetration depth and minimum health risks. Herein, we disclose a red-light (λ = 640 nm)-mediated C-3 formylation of indoles utilizing a helical carbenium ion as a photocatalyst and 2,2-dimethoxy-N,N-dimethylethanamine as a formylating source. These protocols exhibit a broad substrate scope under mild conditions with efficient scalability for the synthesis of C-3 formylated indoles.
72.	Risk assessment of particle and gaseous emissions from diesel and methanol–diesel advanced dual-fuel engines **NK Yadav, RK Maurya** - Biofuels, 2025 **Abstract:** The study investigates the influence of engine load and methanol energy share on the ultrafine particulate matter (PM) and unregulated emissions from advanced dual-fuel (reactivity-controlled compression ignition (RCCI)) and conventional diesel combustion (CDC) engines. An automotive diesel engine was modified to operate in RCCI mode by integrating a port fuel injection system with methanol. Real-time PM and gas-phase emissions were measured using a DMS 500 particle sizer and FTIR (Fourier-Transform Infra-Red) emission analyser. The study aims to evaluate the effect of combustion modes and operating conditions on exhaust emissions and their effect on human health and the environment. A comprehensive toxicity assessment was conducted which included quantifying the cytotoxicity on BEAS-2B epithelial lung cells exposed to PM, assessing lung retention of PM particles due to inhalation, and determining the cancer risk potential from carbonyl emissions. The risk assessment findings show that RCCI engine-emitted PM particles exhibit lower lung retention than those from the CDC engine. Furthermore, the environmental impact assessment reveals that RCCI engines emit unregulated emissions and exhibit lower global warming potential, acidification potential, and eutrophication potential than CDC engines. Notably, RCCI engines that emitted unsaturated HCs (Hydrocarbons) and carbonyl emissions show higher ozone-forming potential and cancer risk potential.
73.	Robust peer-to-peer federated learning for non-intrusive load monitoring in smart homes **V Agarwal**, O Ardakanian, **S Pal** - Energy and Buildings, 2025 **Abstract:** This paper presents a robust peer-to-peer federated learning (P2P-FL) framework for training a deep learning model for non-intrusive load monitoring (NILM) in smart homes. The main motivation for developing P2P-FL is that NILM datasets contain aggregate and individual plug measurements, which could reveal sensitive information about each household. P2P-FL eliminates the need to centralize private training data and removes the single trusted entity that performs aggregation in FL, allowing privacy-preserving model training. To enhance its robustness to malicious nodes in the peer-to-peer network, we propose a novel aggregation strategy that takes into account the pairwise similarity score and the accuracy of the received model from each peer. The similarity score is computed in a privacy-preserving manner using the Blind RSA-based private set intersection protocol in conjunction with the Jaccard index. Using a state-of-the-art bidirectional transformer architecture as our NILM model, we evaluate P2P-FL on real-world NILM datasets showing its efficacy compared to conventional FL.
74.	Room-temperature-operated Fe_2O_3/PANI-based flexible and eco-friendly ammonia sensor with sub-ppm detectability A Beniwal, **R Gond**, X Karagiorgis, **B Rawat**, C Li - IEEE Sensors Letters, 2025

Abstract: In this letter, a room temperature (RT) (~27 °C) operated ferric oxide/polyaniline (Fe_2O_3/PANI) composite-based flexible ammonia sensor with substantial sensing performance is reported. Initially, interdigitated electrodes were screen printed (using graphene-carbon-based ink) on a bio-degradable paper substrate. Further, PANI nanofibers were electrospun on printed IDEs, followed by drop casting a layer of Fe_2O_3. X-ray diffraction and Fourier transform infrared spectroscopy studies were performed to confirm the composite formation, followed by scanning electron microscopy analysis to examine the sensing surface morphology. The ammonia sensing performance was examined within the range of 0.5 ppm (i.e., 500 ppb) to 50 ppm, with a 1.99% response achieved even at 0.5 ppm. The response/recovery times were noted as 950/250 s toward 0.5 ppm of ammonia. In addition, selectivity toward interference gases including carbon dioxide, nitrogen dioxide, carbon monoxide, and sulfur dioxide was also investigated. The proposed sensing mechanism of the composite material toward ammonia gas detection is also presented.

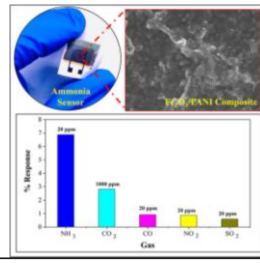

75.

[Ruthenium-catalyzed intramolecular allene–alkyne cascade cyclization: access to the sulfone-cyclopenta[a]naphthalene core]

P Singh, Deepshikha, N Lal, MV Mane, **AC Shaikh** - Organic Letters, 2025

Abstract: A ruthenium-catalyzed intramolecular cascade cyclization of allene–alkyne has been achieved. This method offers a streamlined and atom-economical approach for the construction of sulfone bearing 1H-cyclopenta[a]naphthalenes, an important structural scaffold that exists in biologically active compounds. Our approach, backed by mechanistic insights from deuterium labeling, DFT calculations, and potential for reaction scale-up, presents synthetic chemists with an invaluable tool for efficiently producing a distinct carbon framework in a one-pot manner. This protocol is operationally simple, exhibiting a broad substrate scope with consistently high yields.

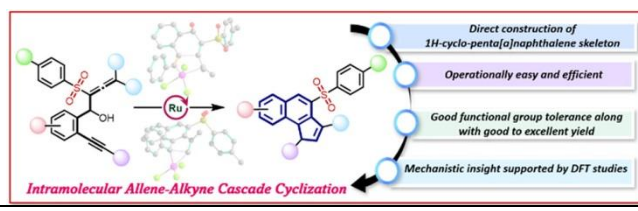

76.

[SecureTrack: Protecting vehicular sensors from non-invasive emi attacks]

RK Singh, S Mishra - IEEE Sensors Journal, 2025

Abstract: The automotive industry's advancements in road safety through sensors, actuators, and customized networks are challenged by increasing accidents, particularly in vehicles operating in Autopilot mode. A significant concern is the ability to tamper with sensor data through low-power electromagnetic interference (EMI) without physical contact. Our research focuses on the physical layer of vehicular networks, investigating the risk of misleading sensor data caused by deliberate EMI targeting critical subsystems. Through experiments on ultrasonic and crankshaft sensors, we developed an EMI Injection Unit and Detection Unit to evaluate the potential for sensor hacking and its impact on vehicle safety. Our findings reveal that current onboard diagnostics (OBDs) cannot detect these EMI-based attacks. To address this gap, we propose SecureTrack, an EMI detection and alert system that effectively identifies interference attempts in real-time. Using a micro-antenna system and an embedded AVR microcontroller, our system

	measures EMI strength and resonant voltage. Furthermore, IoT-based integration enhances vehicle safety by enabling OBD and central control centres to tackle such threats. To the best of our knowledge, this is the first system developed to detect and alert against EMI attacks on automotive sensors, marking a significant advancement in the field of vehicular security.
77.	Seismic evaluation of open ground storey RC buildings with realistic functional openings in upper storey infills **PL Kurmi, P Haldar** - Structures, 2025 **Abstract:** Multi storey Reinforced Concrete (RC) buildings with Un-Reinforced Masonry (URM) infills as partition walls are gaining enormous popularity in India and around the world. Often, the ground storey of these buildings is kept free from any partition walls referred as Open Ground Storey (OGS) to use as parking space/commercial purposes. However, the devastating consequences of poor seismic performance of URM infilled OGS RC buildings, even in moderate earthquakes in recent past, have stirred up the concern regarding seismic safety of this preferred OGS buildings. Several studies have been undertaken on the structural design and retrofitting techniques of OGS buildings; however, effect of functional openings in terms of doors and windows present in the upper storey infills in the OGS building have been ignored. Although, it has been well established, that openings in infills significantly affect seismic behaviour of infilled frame buildings, unfortunately, insignificant efforts have been devoted to understand the seismic response and governing failure mechanism of OGS buildings with realistic combination of functional openings in upper storey infills. Present study evaluates the influence of functional opening in upper storey infills on seismic performance and failure mechanism of URM infilled OGS RC buildings of varying design levels. Extensive analytical studies have been carried out on a set of mid and high-rise OGS RC frame buildings considering various realistic combinations of functional openings. The study indicates that presence of functional opening in infills at upper storey levels significantly degrades the seismic performance of OGS buildings in terms of strength, stiffness, ductility whereas upgrades plastic deformation capacity. Ductility of OGS buildings are found to be very sensitive with increasing functional opening. Functional openings are integral part of residential building and cannot be avoided completely. Therefore, based on the study, 15 % opening can be considered as optimum percentage of opening in the building where the strength and ductility can be achieved up to 80 % of its ideal counterpart OGS buildings with solid upper storey infills.
78.	Some complexity results on semipaired domination in graphs V Tripathi, **Kusum, A Pandey** - AKCE International Journal of Graphs and Combinatorics, 2024 **Abstract:** Let $G=(V,E)$ be a graph without any isolated vertices. A semipaired dominating set $D\subseteq V$ of G, is a dominating set of G, if D can be partitioned into cardinality 2 subsets such that the vertices in each of these subsets are at distance at most two from each other. The Min-Semi-PD problem is to compute a minimum cardinality semipaired dominating set of a given graph G. It is known that the decision version of the problem is NP-complete for bipartite graphs and split graphs. In this article, we resolve the complexity of the problem in two well studied graph classes, namely, AT-free graphs and planar graphs. We show that the decision version of the Min-Semi-PD problem remains NP-complete for planar graphs. On the positive side, we propose a polynomial-time exact algorithm for the Min-Semi-PD problem in AT-free graphs, but the complexity of the algorithm is quite high. So, in addition, we also give a linear-time constant factor approximation algorithm for the problem in AT-free graphs.
79.	Surface engineered nanoparticles coupled with pattern recognition techniques for rapid identification and discrimination of multiple thiols in a real sample matrix **L Sharma, Ranbir, G Singh**, N Kaur, **N Singh** - Analytical Chemistry, 2025 **Abstract:** Thiols, including Cysteine (CYS) and Glutathione (GSH), play pivotal roles in

	numerous physiological processes as they are integral components of many essential biomolecules and are found abundantly in foods such as additives and antioxidants. Any deviations in thiol concentrations can disrupt normal physiological functions, affecting the body's metabolism and potentially leading to diseases such as Alzheimer's and Parkinson's diseases, etc. Consequently, the imperative need for developing reliable and robust techniques for thiol analysis is crucial for early disease detection and ensuring food safety. In this regard, we have decorated the surface of organic nanoparticles with metal ions, which have been characterized using various techniques such as Dynamic Light Scattering (DLS), Zeta potential, Fourier Transformation Infrared Spectroscopy (FTIR), X-ray Photoelectron Spectroscopy (XPS), and Transmission Electron Microscopy (TEM) and utilized for the detection and discrimination of various thiols (cysteine, Glutathione, 3-mercaptopropionic acid, 2-mercapto ethanol, and cysteamine). Photophysical results revealed that various thiols exhibit unique binding affinities toward sensor elements, serving as fingerprints for each thiol. These patterns can be quantitatively differentiated using linear discrimination analysis (LDA) and hierarchical clustering analysis (HCA). The sensor array effectively discriminates target thiols with 100% accuracy and high sensitivity with limit of detection values from 1.19 to 4.20 μM. Apparently, it offers required simplicity, rapid response, sensitivity, and stability, which holds promise for enhancing food safety. 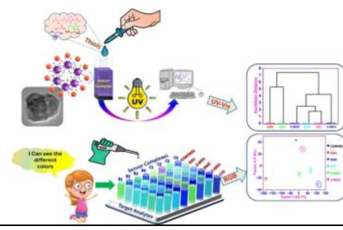
80.	[Tipping events in a fear-affected symbiotic ecological system with adaptive hunting strategy] M Kausar Sk, **A Mandal**, J Chattopadhyay - Chaos: An Interdisciplinary Journal of Nonlinear Science, 2025 **Abstract:** Experimental observations and field data demonstrated that predators adapt their hunting strategies in response to prey abundance. While previous studies explored the impact of predation risk on predator–prey interactions, the impact of symbiotic relationships between fear-affected prey and non-prey species on system dynamics remains unexplored. This study uses a mathematical approach to investigate how different symbiotic relationships govern system dynamics when predators adapt to prey availability. Our study illustrates that the mutualistic relationship between prey and partners extends predator survivability. However, the fear-affected symbiotic system may undergo regime shifts, which can be catastrophic or non-catastrophic, depending on symbiotic interaction patterns. The study demonstrates a hump-shaped relationship between the predator's optimal search rate and biomass and identifies an intermediate range of search rates where the system exhibits a "bubbling"phenomenon. Overall, our findings provide new insights into symbiotic relationships in community ecology, highlighting the complex interplay among predators, prey, and non-prey species.
81.	[Violence and taoist ethics in Ursula K. Le Guin's The Word for World is Forest] **AA Paul**, S Krishna S - UKL: The Journal of Ursula K. Le Guin Studies, 2025 **Abstract:** This note critically investigates the ethico-moral intricacies of violence/peace in Ursula K. Le Guin's *The Word for World is Forest* (1976) while arguing that her radical political sensibilities are informed by her ardent Taoist worldview. Amidst the urgent tussle for domination by the colonizing Terrans and the struggle for survival by the native Athsheans in the fictional planet Athshe, Le Guin incorporates her incisive critique of imperialist exploitation and militarism while upholding the non-dualistic ethics of Taoism. Moving beyond the moral imperatives and either/or debates, Le Guin illustrates how from time-to-time violence turns to be the singular means of self-preservation for persecuted communities, thereby resolving the glaring

	opposition between violence and peace in the novella.

Disclaimer: This publication digest may not contain all the papers published. Library has compiled the publication data as per the alerts received from Scopus and Google Scholar for the affiliation "Indian Institute of Technology Ropar" for the month of January, 2025. The author(s) are requested to share their missing paper(s) details if any, for the inclusion in the next publication digest.